Toxicology Letters 206 (2011) 152–157

Contents lists available at ScienceDirect

Toxicology Letters

journal homepage: www.elsevier.com/locate/toxlet

Xenoestrogens down-regulate aryl-hydrocarbon receptor nuclear translocator 2 mRNA expression in human breast cancer cells via an estrogen receptor alpha-dependent mechanism

Xian-Yang Qin[a,b], Hiroko Zaha[a], Reiko Nagano[a], Jun Yoshinaga[b], Junzo Yonemoto[a], Hideko Sone[a,*]

[a] Research Center for Environmental Risk, National Institute for Environmental Studies, 16-2 Onogawa, Tsukuba 305-8506, Japan
[b] Department of Environmental Studies, The University of Tokyo, Kashiwanoha 5-1-5, Kashiwa, Chiba 270-8563, Japan

ARTICLE INFO

Article history:
Received 20 January 2011
Received in revised form 1 July 2011
Accepted 4 July 2011
Available online 12 July 2011

Keywords:
ARNT2
Xenoestrogen
E-CALUX
Endocrine disruption
Tumorigenesis

ABSTRACT

Environmental chemicals with estrogenic activity, known as xenoestrogens, may cause impaired reproductive development and endocrine-related cancers in humans by disrupting endocrine functions. Aryl-hydrocarbon receptor nuclear translocator 2 (ARNT2) is believed to play important roles in a variety of physiological processes, including estrogen signaling pathways, that may be involved in the pathogenesis and therapeutic responses of endocrine-related cancers. However, much of the underlying mechanism remains unknown. In this study, we investigated whether ARNT2 expression is regulated by a range of representative xenoestrogens in human cancer cell lines. Bisphenol A (BPA), benzyl butyl phthalate (BBP), and 1,1,1-trichloro-2,2-bis(2-chlorophenyl-4-chlorophenyl)ethane (*o,p'*-DDT) were found to be estrogenic toward BG1Luc4E2 cells by an E-CALUX bioassay. ARNT2 expression was downregulated by BPA, BBP, and *o,p'*-DDT in a dose-dependent manner in estrogen receptor 1 (ESR1)-positive MCF-7 and BG1Luc4E2 cells, but not in estrogen receptor-negative LNCaP cells. The reduction in ARNT2 expression in cells treated with the xenoestrogens was fully recovered by the addition of a specific ESR1 antagonist, MPP. In conclusion, we have shown for the first time that ARNT2 expression is modulated by xenoestrogens by an ESR1-dependent mechanism in MCF-7 breast cancer cells.

1. Introduction

Environmental chemicals with estrogenic activity, known as xenoestrogens, are currently the largest group of known endocrine disruptors (EDs) (Welshons et al., 2003). Over the past few decades, a considerable number of publications have indicated that maternal exposure to EDs may cause impaired reproductive development and endocrine-related cancers in humans by disrupting endocrine functions. Concerns have been focused on a variety of environmental chemicals, including bisphenol A (BPA), phthalates, organochlorine pesticides, dioxin and polychlorinated biphenyls and their hydroxylated metabolites (OH-PCBs). However, the findings remain controversial (Safe, 2004; Sharpe and Irvine, 2004; Sikka and Wang, 2008). An excellent example of an ED is diethylstilbestrol (DES), a synthetic estrogen that was administered to pregnant women to prevent miscarriage during the 1940s and 1970s. It is currently well understood that prenatal exposure to DES may be associated with adverse pregnancy outcomes, genital tract abnormalities, infertility, and vaginal and cervical cancers (Hatch et al., 2010; Ma, 2009).

Aryl-hydrocarbon receptor nuclear translocator 2 (ARNT2) is a member of the basic helix-loop-helix Per-ARNT-SIM (bHLH-PAS) family of transcription factors (Hirose et al., 1996) and acts as a common obligate partner for several other members of the family, including aryl hydrocarbon receptor (AHR) and hypoxia-inducible factor (HIF)-1α (Hankinson, 2008; Sekine et al., 2006). ARNT2 knockout mice suffer severe developmental defects and die shortly after birth (Hosoya et al., 2001). Similar findings were observed in the zebrafish (Hsu et al., 2001). Although many of the functions of ARNT2 remain unknown, it is believed that ARTN2 may play important roles in tumor angiogenesis (Maltepe et al., 2000) and many physiological pathways, including the responses to environmental contaminants, oxygen deprivation, biological rhythms, angiogenesis, and neuronal development (Hill et al., 2009). In addition, a recent epidemiological study found that ARNT2 expression was correlated with the prognosis of breast cancer patients by participating in the metabolism of certain environmental chemicals, indicating potential interactions between ARNT2 and estrogen receptor (ER) signaling pathways (Martinez et al., 2008).

In this study, we investigated the effects of xenoestrogens on ARNT2 expression in two estrogen-dependent cancer cell lines,

* Corresponding author. Tel.: +81 29 850 2546; fax: +81 29 850 2546.
E-mail address: hsone@nies.go.jp (H. Sone).

0378-4274/$ – see front matter © 2011 Elsevier Ireland Ltd. All rights reserved.
doi:10.1016/j.toxlet.2011.07.007

MCF-7 human breast cancer cells and BG1Luc4E2 human ovarian cancer cells, and one estrogen-independent cancer cell line, LNCaP human prostate cancer cells. The estrogenic activities of a range of representative EDs were measured using an estrogenic chemically activated luciferase gene expression (E-CALUX) bioassay. We also examined the mechanism of ARNT2 regulation, in terms of the ER-dependent activation pathway.

2. Materials and methods

2.1. Chemicals

Dimethyl sulfoxide (DMSO) and 17β-estradiol (E2) were obtained from Sigma Chemical Co. (St. Louis, MO). 1,3-Bis(4-hydroxyphenyl)-4-methyl-5-[4-(2-piperidinylethoxy)phenol]-1H-pyrazole dihydrochloride (MPP) was obtained from Tocris (Ellisville, MO). DMSO was used as the primary solvent for all chemicals, and the DMSO solutions were further diluted in cell culture media for treatments. The final concentrations of DMSO in the media did not exceed 0.1% (vol/vol).

BPA, benzyl butyl phthalate (BBP), di-*n*-butyl phthalate (DBP), and di(2-ethylhexyl) phthalate (DEHP) were obtained from Wako Industries (Osaka, Japan). 2,3,3′,4′,5-Pentachloro-4-biphenylol (OH-PCB 107), 2,2′,3,4′,5,5′-hexachloro-4-biphenylol (OH-PCB 146), and 2,2′,3,4′,5,5′,6-heptachloro-4-biphenylol (OH-PCB 187) were obtained from Wellington Laboratories (Guelph, ON, Canada). 2,3,7,8-Tetrachlorodibenzo-*p*-dioxin (TCDD) was obtained from Cambridge Isotope Laboratories (Cambridge, MA). 1,1,1-Trichloro-2,2-bis(4-chlorophenyl)ethane (*p,p′*-DDT) and 1,1,1-trichloro-2,2-bis(2-chlorophenyl-4-chlorophenyl)ethane (*o,p′*-DDT) were obtained from AccuStandard (New Haven, CT).

2.2. Cell culture

MCF-7 and LNCaP cells were obtained from the Cell Engineering Division of RIKEN BioResource Center (Tsukuba, Ibaraki, Japan). The BG1Luc4E2 cells used in the E-CALUX bioassay were a gift from Dr. M. Denison (University of California, Davis, CA). The estrogen receptor 1 (ESR1)-positive BG1Luc4E2 cells are BG-1 ovarian cancer cells stably transfected with a luciferase reporter gene under the control of estrogen response element (ERE) that is responsive to the exposure to estrogen or estrogenic chemicals (Rogers and Denison, 2000). MCF-7, LNCaP, and BG1Luc4E2 cells were maintained in RPMI 1640 medium (Wako, Osaka, Japan) containing 10%, 10%, and 8% fetal bovine serum (FBS) (Mediatech, Herndon, VA), respectively. All of the cells were grown at 37 °C in a 5% CO_2 humidified incubator. For growth under steroid-free conditions, the cells were seeded in phenol red-free DMEM (MP Biomedicals, Solon, OH) containing 5% charcoal/dextran-treated FBS (Hyclone, Logan, UT). All the culture media contained 100 U/ml penicillin/streptomycin and 2 mmol/L L-glutamine (Mediatech, Herndon, VA).

2.3. Luciferase assay

BG1Luc4E2 cells were plated in 96-well plates (4×10^4 cells/well) and cultured under steroid-free conditions for 24 h, before exposure to EDs for 24 h. After removal of the medium, the plates were rinsed with phosphate-buffered saline (Gibco, Grand Island, NY), and the cells were lysed with 20 μl/well lysis buffer (Promega, Madison, WI). The luciferase activity was measured in an AB-2100 luminometer (Atto, Tokyo, Japan) after the addition of 100 μl/well luciferase assay reagent (Promega) and expressed as relative light units. Luciferase induction was calculated as a percentage of the vehicle control by setting the induction by DMSO at 100%. The half-maximal effective concentration, EC_{50}, was calculated for each test compound using a previously described method (Alexander et al., 1999).

2.4. Quantitative real-time reverse transcription-polymerase chain reaction (RT-PCR)

Total RNA for real-time RT-PCR was isolated from the three cell lines after treatment with the EDs for 24 h using an RNeasy Kit (Qiagen, Valencia, CA) in accordance with the manufacturer's instructions. Quantification and quality assessment of the isolated RNA samples were performed and verified using an Agilent Bioanalyzer 2100 and an RNA 6000 Nano Assay (Agilent Technologies, Palo Alto, CA) in accordance with the manufacturer's instructions. RNA (9 μg) was transcribed using a High Capacity RNA-to-cDNA Kit (Applied Biosystems, Foster City, CA) according to the manufacturer's instructions. The resulting cDNA (1 μl) was amplified in triplicate using TaqMan® Gene Expression Master Mix (Applied Biosystems) in accordance with the manufacturer's instructions. TaqMan® Gene Expression Assays (Applied Biosystems) used in this study were Hs00208298_m1 for *ARNT2*, Hs00420042_m1 for PDZ domain containing 1 (*PDZK1*), and Hs00266705_g1 for glyceraldehyde-3-phosphate dehydrogenase (*GAPDH*). The amplification reaction was performed in an ABI PRISM 7000 Sequence Detector (Applied Biosystems) under the following cycling conditions: 95 °C for 15 min, followed by 40 cycles of 95 °C for 15 s and 60 °C for 60 s. The gene expression levels were calculated based on the threshold cycle using Sequence Detection System Software (Applied Biosystems). The gene expression was normalized by the GAPDH expression and set to 1 for the control DMSO-treated cells.

2.5. Western blot analysis

To evaluate the effects of EDs exposure on ARNT2 protein expression, Western blot was performed using the polyclonal anti-ARNT2 M-165 antibody from Santa Cruz Biotechnology (sc-5581, 1:500 dilution, Santa Cruz, CA). MCF-7 cells (2.5×10^6) treated with EDs were lysed using RIPA buffer solution (Santa Cruz Biotechnology). After boiling at 99 °C for 5 min, the protein samples were resolved by SDS polyacrylamide gel electrophoresis on a 10% gel and transferred to a polyvinylidene difluoride membrane (Bio-Rad Laboratories, Hercules, CA). After blotting in TBS with 5% nonfat dry milk–Tris buffered saline and 0.1% Tween, the membrane was probed with Actin H-196 (sc-7210, 1:500 dilution, Santa Cruz Biotechnology) or ARNT2 M-165 primary antibody. Blots were then incubated with a horseradish peroxidase (HRP)-conjugated anti-rabbit secondary antibody (ECL plus Western blotting reagent pack, RPN2124, 1:10,000 dilution, GE Healthcare UK, Buckingham, England). The immune complex was detected with the Amersham ECL Plus™ Western Blotting Detection System (RPN2132, GE Healthcare UK). The blots were exposed to Hyperfilm (Amersham Pharmacia Biotech), and bands were quantified with ImageJ densitometry software (National Institutes of Health, Bethesda, MD).

2.6. Statistical analysis

All experiments in this study were performed in triplicates to test the reproducibility of the results. Quantitative data were expressed as the means ± SD. The statistical significance of differences between values was assessed using a two-tailed Student's *t*-test. Values of $P < 0.05$ were considered to indicate statistical significance.

3. Results

3.1. Estrogenic activities of EDs toward BG1Luc4E2 cells

The effects of E2 and several EDs on ESR1-mediated luciferase induction were measured by an E-CALUX bioassay in the human ovarian cancer cell line BG1Luc4E2 (Fig. 1 and Table 1). E2 significantly increased the ESR1-induced luciferase activity in a dose-dependent manner compared with the control DMSO-treated

Table 1
Estrogenic activity of EDs in the E-CALUX bioassay.

Chemicals	LOEC (M)	EC_{50} (M)	MOEC (M)	% of control (max)
E2	4.1×10^{-13}	4.8×10^{-13}	1×10^{-10}	263
BPA	1.23×10^{-7}	2×10^{-7}	3.33×10^{-6}	220
BBP	1.23×10^{-7}	2.45×10^{-7}	1×10^{-5}	295
DBP	–	–	–	–
DEHP	–	–	–	–
o,p′-DDT	3.13×10^{-7}	8.92×10^{-7}	5×10^{-6}	285
p,p′-DDT	3.13×10^{-7}	nd	5×10^{-6}	175
OH-PCB107	1.4×10^{-7}	nd	1.4×10^{-7}	117
OH-PCB146	2.3×10^{-10}	nd	1.3×10^{-7}	122
OH-PCB187	4.8×10^{-8}	nd	2.4×10^{-8}	125
TCDD	4.96×10^{-11}	6.0×10^{-10}	1.55×10^{-7}	43

LOEC, lowest observed effect concentration; EC_{50}, half of maximum effect concentration; MOEC, maximum observed effect concentration; –, no effect observed; nd, not determined; M, mol/L.

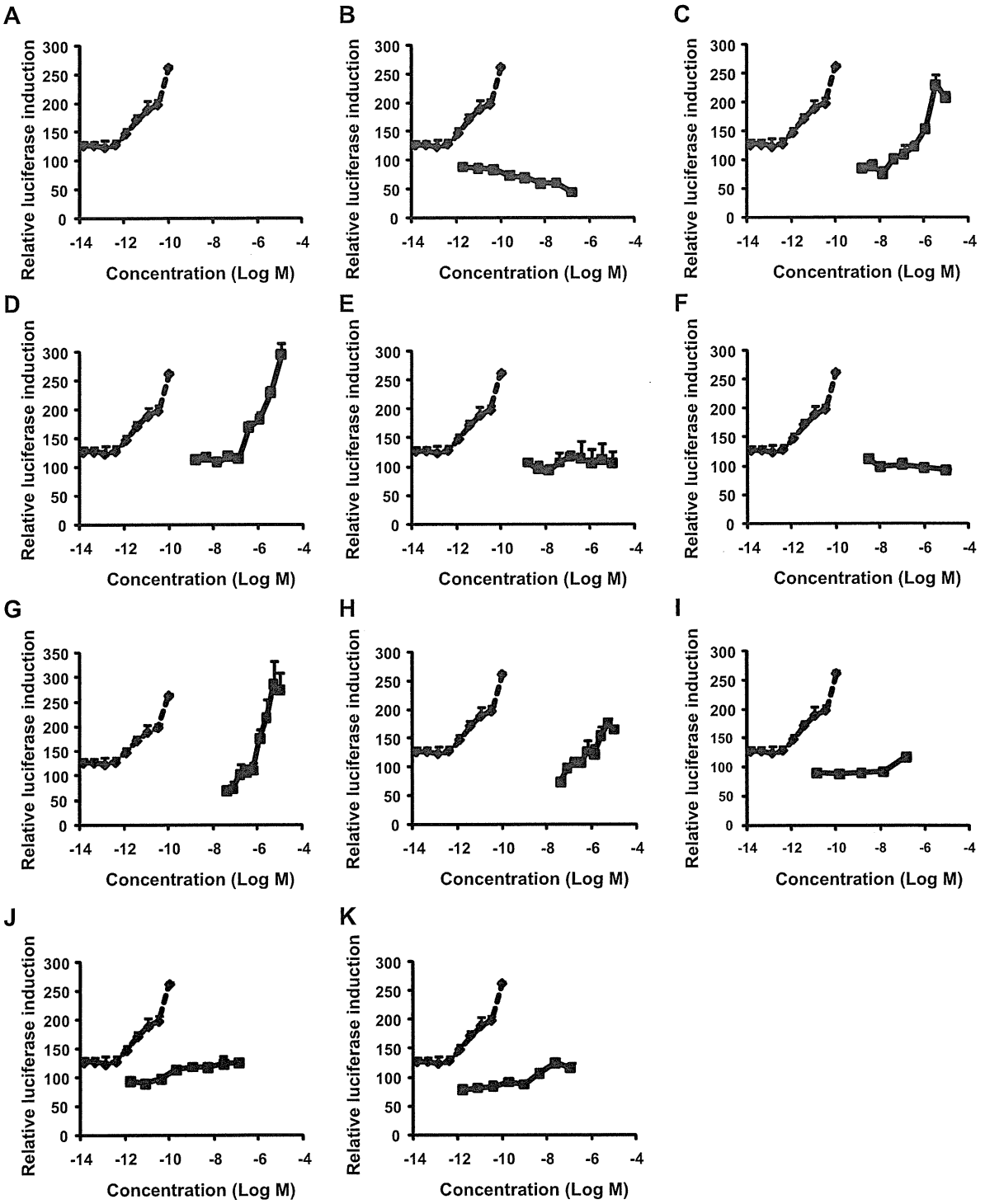

Fig. 1. Effects of xenoestrogens on the induction of ESR1-induced luciferase activity in the E-CALUX bioassay. BG1Luc4E2 cells were treated with E2 (A), TCDD (B), BPA (C), BBP (D), DBP (E), DEHP (F), *o,p′*-DDT (G), *p,p′*-DDT (H), OH-PCB107 (I), OH-PCB146 (J), and OH-PCB187 (K) at increasing concentrations for 24 h. All the data are expressed as the percentage of the vehicle control (DMSO) treatment. Each value is the mean ± SD of a representative experiment performed in triplicate. The data for E2 (dotted lines) are shown in all the compound charts for comparison.

cells, with maximal stimulation at 10^{-10} M. Among the EDs, BPA, BBP, and *o,p′*-DDT increased the ESR1-induced luciferase activity in a dose-dependent manner at 10^{-7} M to 10^{-5} M for BPA and *o,p′*-DDT, and at 10^{-8} M to 10^{-5} M for BBP. Weak, but significant, effects were observed for *p,p′*-DDT and OH-PCB107 at 10^{-5} M and 10^{-7} M, respectively. No significant effects were observed for DBP, DEHP, OH-PCB146, or OH-PCB187. TCDD, a well-known AHR ligand, significantly decreased the ESR1-induced luciferase activity in a dose-dependent manner at 5×10^{-11} M to 10^{-7} M. These results suggest that the EDs BPA, BBP, and *o,p′*-DDT may act as ESR1 agonists.

3.2. Modulation of ARNT2 expression by xenoestrogens in MCF-7, BG1Luc4E2, and LNCaP cells

The estrogenic effects of xenoestrogens are primarily mediated by ERs, including ESR1 and estrogen receptor 2 (ESR2) (Watanabe

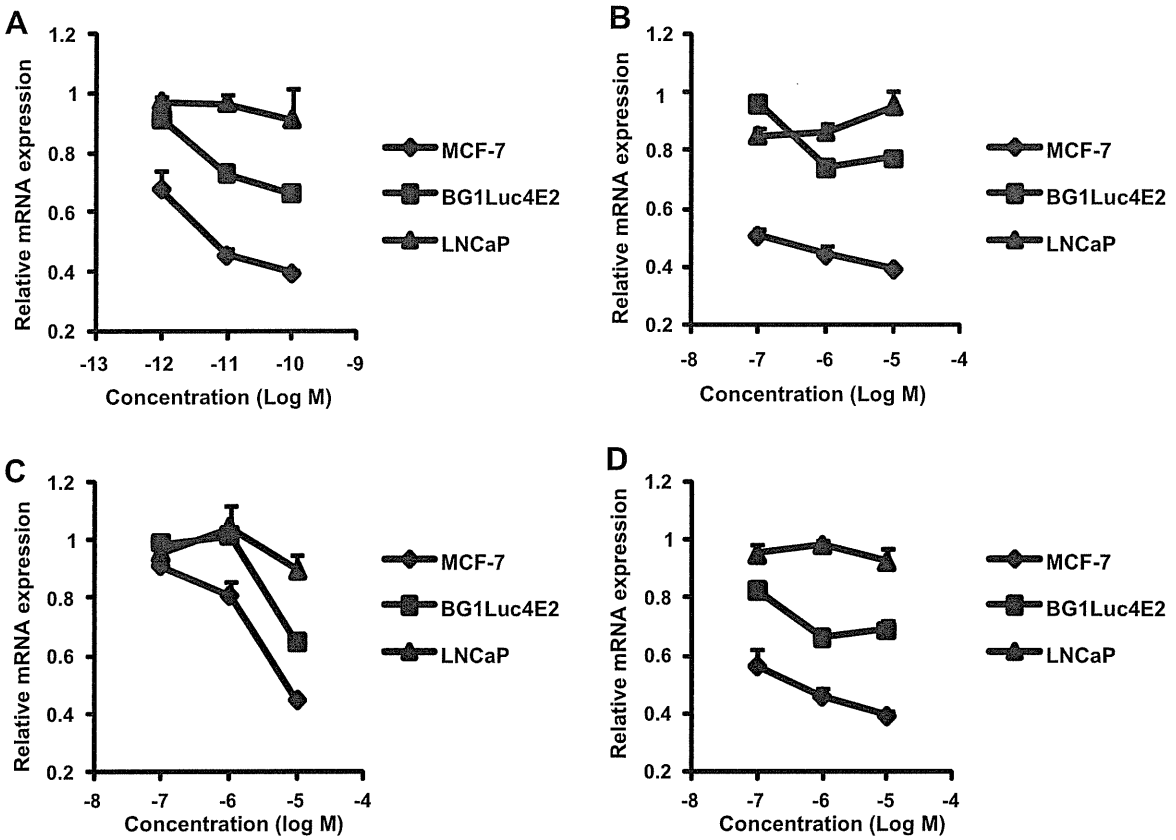

Fig. 2. Modulation of ARNT2 mRNA expression in MCF-7, BG1Luc4E2, and LNCaP cells by xenoestrogens. Cells were treated with DMSO or increasing concentrations of E2 (A), BPA (B), BBP (C), or *o,p′*-DDT (D) for 24 h. All the data are expressed as the fold induction relative to the vehicle control (DMSO) treatment. Each value is the mean ± SD of a representative experiment performed in triplicate.

et al., 2007). Since the presence of these two ER subtypes may contribute to differences in the binding affinities of certain compounds and the subsequent activation of gene expression in various tissues, we examined whether MCF-7, BG1Luc4E2, and LNCaP cells expressed ESR1 and ESR2. The presence of ESR1 mRNA in MCF-7 and BG1Luc4E2 cells and the absence of both ESR1 and ESR2 mRNAs in LNCaP cells were confirmed by real-time RT-PCR (data not shown).

To investigate the abilities of xenoestrogens to modulate ARNT2 expression, MCF-7, BG1Luc4E2, and LNCaP cells were treated for 24 h with E2 and different xenoestrogens at increasing concentrations that induced the minimal, median, and maximal luciferase activities in the E-CALUX bioassay (see Table 1). The expression level of ARNT2 mRNA was determined by quantitative real-time RT-PCR (Fig. 2). E2 and the xenoestrogens BPA, BBP, and *o,p′*-DDT significantly decreased ARNT2 expression in ESR1-positive MCF-7 and BG1Luc4E2 cells in a dose-dependent manner. E2 was able to decrease ARNT2 expression at low concentrations of 10^{-12} to 10^{-10} M (0.39-fold and 0.66-fold reduction at 10^{-10} M in MCF-7 and BG1Luc4E2 cells, respectively; Fig. 2A). Maximal effects were observed at 10^{-5} M for BPA, BBP, and *o,p′*-DDT (0.39-fold and 0.78-fold reduction for BPA, 0.45-fold and 0.65-fold reduction for BBP, and 0.39-fold and 0.69-fold reduction for *o,p′*-DDT in MCF-7 and BG1Luc4E2 cells, respectively; Fig. 2B-D). No significant effects were observed in ER-negative LNCaP cells for any of the chemical compounds (Fig. 2).

We also investigated the effects of E2 and xenoestrogens exposure on ARNT2 protein expression in MCF-7 cells using Western blot analysis. As shown in Fig. 3, significant decreases in ARNT2 protein levels were observed following E2 and xenoestrogens BPA, BBP, and *o,p′*-DDT treatments.

3.3. The modulation of ARNT2 expression in MCF-7 cells by xenoestrogens is ESR1-dependent

Next, we investigated whether the xenoestrogens decreased ARNT2 expression in MCF-7 cells in an ESR1-dependent manner.

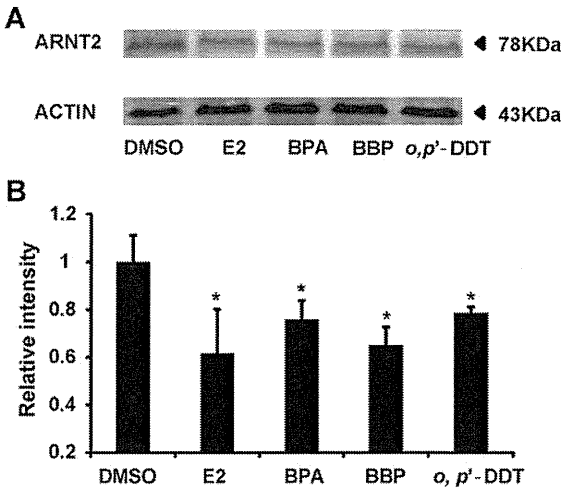

Fig. 3. Modulation of ARNT2 protein expression in MCF-7 cells by xenoestrogens. (A) Cells were treated with DMSO, 0.1 nM E2, 10 μM BPA, 10 μM BBP, or 10 μM *o,p′*-DDT for 24 h, and then analyzed by Western blot. (B) The cellular protein levels of ARNT2 were calculated using ImageJ densitometry software and are expressed as the mean ± SD relative to vehicle control (DMSO) after normalizing the bands to ACTIN. Representative data were shown from triplicate experiments. *$P < 0.05$ vs. the vehicle control (DMSO).

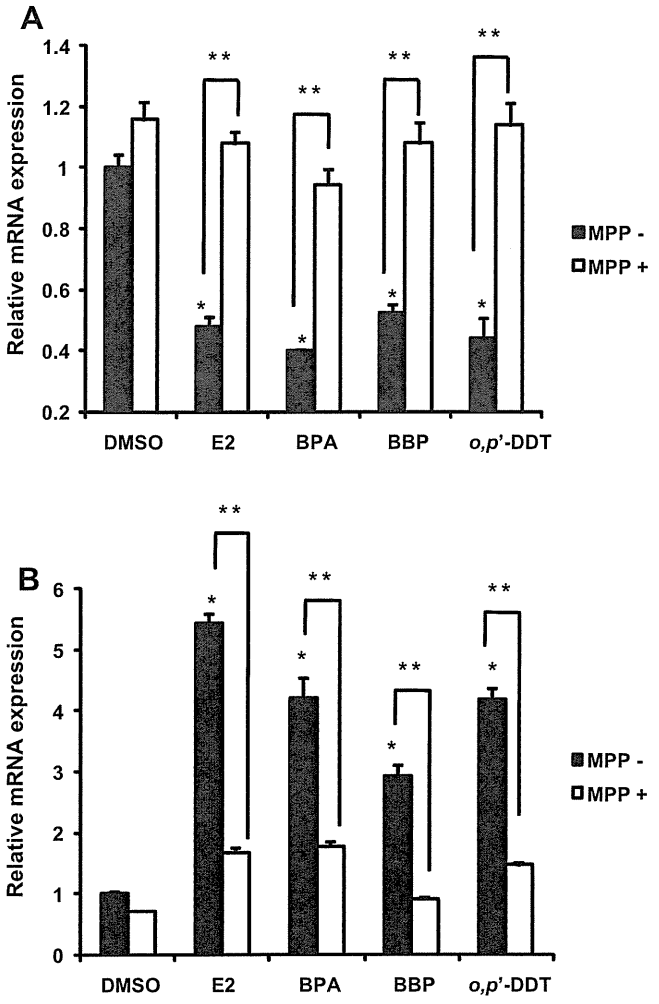

Fig. 4. ARNT2 mRNA expression decrease mediated by xenoestrogens is increased by MPP in breast cancer cells. MPP, an ESR1 antagonist, blocks the ability of xenoestrogens to modulate ARNT2 (A) and PDZK1 (B) expression in MCF-7 cells. Cells were treated with DMSO, 0.1 nM E2, 10 μM BPA, 10 μM BBP, or 10 μM *o,p'*-DDT for 24 h alone or in combination with 0.1 μM MPP. All the data are expressed as the fold induction relative to the vehicle control (DMSO) treatment. Each value is the mean ± SD of a representative experiment performed in triplicate. $^{*}P < 0.05$ vs. the vehicle control, $^{**}P < 0.05$ vs. the corresponding xenoestrogen control.

To achieve this, we examined the effects of the specific ESR1 antagonist MPP, which has been shown to selectively block ESR1- but not ESR2-mediated transactivation (Harrington et al., 2003). As shown in Fig. 4A, the decrease in ARNT2 expression was significantly inhibited in MCF-7 cells after the addition of MPP in the presence of E2, BPA, BBP, and *o,p'*-DDT. PDZK1, a well-known estrogen-regulated gene expressed in hormone-responsive breast cancer (Ghosh et al., 2000), was used as a positive control in this experiment. As shown in Fig. 4B, E2 at 10^{-10} M, and BPA, BBP, and *o,p'*-DDT at 10^{-5} M significantly increased PDZK1 expression (5.4-fold, 4.2-fold, 2.9-fold, and 4.2-fold induction, respectively). The levels of PDZK1 mRNA after stimulation with E2 and xenoestrogens were fully recovered in the presence of the specific ESR1 antagonist MPP. Taken together, these findings indicate that the modulatory effects of xenoestrogens on ARNT2 expression are dependent on ESR1-mediated pathways.

4. Discussion

In this present study, we have shown that xenoestrogens significantly decrease ARNT2 expression in MCF-7 breast cancer cells through an ESR1-dependent pathway. We determined the estrogenic and anti-estrogenic activities of a variety of EDs, including BPA, BBP, *o,p'*-DDT, and TCDD in BG1Luc4E2 ovarian cancer cells by an ERE-luciferase bioassay. Our results are consistent with previous reports in other human cell lines, although the approaches applied for the estrogenic activity measurements differed slightly (Buteau-Lozano et al., 2008; Ghisari and Bonefeld-Jorgensen, 2009; Rogers and Denison, 2002). The previous report that BG1Luc4E2 cells are positive for ESR1 but not ESR2 indicates that these chemicals mediate the expression of the ERE-luciferase gene by ESR1-mediated pathways (Rogers and Denison, 2000). Our findings that xenoestrogens such as BPA, BBP, and *o,p'*-DDT downregulated ARNT2 expression in ESR1-positive MCF-7 and BG1Luc4E2 cells but not in ER-negative LNCaP cells suggest ESR1 may play an important role in the mechanism by which xenoestrogens exert their effects on ARNT2 expression. This notion is further confirmed by the significant inhibition of the xenoestrogen-mediated decrease in ARNT2 expression in MCF-7 cells after the addition of the specific ESR1 antagonist MPP.

Recent research has focused on the roles of ARNT2 in a variety of physiological processes, such as AHR, HIF-1α, and ER signaling pathways, that may be involved in the pathogenesis and therapeutic responses of endocrine-related cancers (Hankinson, 2008; Swedenborg and Pongratz, 2010). However, only two animal studies have attempted to determine the potential effects of E2 on ARNT2 expression in rat models, and their conclusions differed. Mitsushima et al. (2003) described that a subcutaneous injection of E2 increased the expression of Arnt2 mRNA in the mediobasal hypothalamus of ovariectomized rats, while no effects were observed in the preoptic area. In contrast, Kretzschmar et al. (2010) observed downregulation of Arnt2 mRNA expression following a subcutaneous injection of E2 in a dose-dependent manner in the uterus of ovariectomized rats. Although neither of the above-said two studies investigated the underlying mechanism, the differing distributions of the two ER subtypes (ESR1 and ESR2) may account for the different regulations of ARNT2 expression by E2. The presence and relative amounts of each ER subtype may contribute to the differential effects of certain ligands in various tissues, since ESR1 and ESR2 are known to show differences in their relative binding affinities for particular compounds and the subsequent activation of gene expression (Heldring et al., 2007; Kuiper et al., 1997). Our present study provided another evidence that E2 and xenoestrogens might down-regulate ARNT2 mRNA expression in cultured cells. We confirmed the high expression of ESR1 and low expression of ESR2 in human ovarian and breast cancer cells. These results are consistent with previous reports indicating that the ratio of ESR1 to ESR2 (which is normally around one) is altered when ovarian and breast tissues or cells become cancerous, such that ESR1 becomes predominant and ESR2 is dramatically decreased (Brandenberger et al., 1998; Hevir et al., 2011). Furthermore, we found that the suppression of ARNT2 expression after E2 and xenoestrogen treatment was completely reversed in the presence of the specific ESR1 antagonist MPP. Our findings suggest that ESR1-mediated pathways may play principal roles in both ARNT2 expression regulation and the estrogenic activities of xenoestrogens.

To the best of our knowledge, this is the first report that the expression of ARNT2 mRNA is regulated by xenoestrogens in human ESR1-positive cancer cell lines. This may be of particular interest because ARNT2 mRNA expression was reported to be much more prevalent in tumor tissues than in normal tissues and to be significantly correlated with a better prognosis of breast cancer patients (Martinez et al., 2008). An important problem in the treatment of breast cancer patients is that long-term anti-estrogen therapy may result in tumor progression to an estrogen-independent stage and loss of drug sensitivity. Hypoxia is

supposed to be one of the possible factors that promote estrogen-independent growth of breast cancer cells (Scherbakov et al., 2009). ARNT2 protein dimerizes with HIF-1α, and the heterodimer then binds to hypoxia-responsive elements in a variety of responsive genes. These genes may play integral roles in the body's response to low oxygen concentrations or hypoxia and a number of pathological conditions including cancer, heart disease, cerebrovascular disease, and chronic obstructive pulmonary disease (Maltepe et al., 2000; Sekine et al., 2006; Ziello et al., 2007). Our present findings suggest a possible mechanism that downregulation of ARNT2 expression by xenoestrogens may result in the progression of tumors by affecting HIF-1α pathways and endocrine responsiveness and resistance. ARNT2 protein is also assumed to dimerize with AHR, an essential transcription factor in physiologic responses to ubiquitous environmental pollutants and carcinogens that plays an important role in mammary gland tumorigenesis (Schlezinger et al., 2006; Sekine et al., 2006). Our recent findings also indicate a possible mechanism that xenoestrogens may have profound consequences on AHR-mediated detoxification by mediating ARNT2 expression. However, the issue of whether ARTN2 participates in AHR pathways remains controversial (Dougherty and Pollenz, 2008; Hankinson, 2008).

In summary, we have described for the first time that ARNT2 expression is modulated by xenoestrogens in MCF-7 breast cancer cells, in parallel with their estrogenic activity mediated by ESR1 pathways. ARNT2 is believed to be an essential participant in the physiologic responses to many important environmental insults, including chemical toxicants and hypoxia (Hankinson, 2008). The wide exposure to xenoestrogens requires further research to elucidate the functions of the ARNT2 protein in different in vivo and in vitro models in more detail.

Conflict of interest statement

The authors declare that they have no financial or non-financial competing interests.

Acknowledgments

This research was supported by a Grant-in-Aid for Scientific Research from the Ministry of Health, Labour and Welfare of Japan. This research was also partly supported by the Environment Research and Technology Development Fund (C-0905) of the Ministry of the Environment, Japan. We thank Mr. Masafumi Nakamura and Mr. Hiroshi Handa (Hiyoshi Corporation, Omihachiman, Shiga, Japan) for technical support in the estrogenic activity measurements.

References

Alexander, B., Browse, D.J., Reading, S.J., Benjamin, I.S., 1999. A simple and accurate mathematical method for calculation of the EC_{50}. J. Pharmacol. Toxicol. Methods 41, 55–58.

Brandenberger, A.W., Tee, M.K., Jaffe, R.B., 1998. Estrogen receptor alpha (ER-alpha) and beta (ER-beta) mRNAs in normal ovary, ovarian serous cystadenocarcinoma and ovarian cancer cell lines: down-regulation of ER-beta in neoplastic tissues. J. Clin. Endocrinol. Metab. 83, 1025–1028.

Buteau-Lozano, H., Velasco, G., Cristofari, M., Balaguer, P., Perrot-Applanat, M., 2008. Xenoestrogens modulate vascular endothelial growth factor secretion in breast cancer cells through an estrogen receptor-dependent mechanism. J. Endocrinol. 196, 399–412.

Dougherty, E.J., Pollenz, R.S., 2008. Analysis of Ah receptor–ARNT and Ah receptor–ARNT2 complexes in vitro and in cell culture. Toxicol. Sci. 103, 191–206.

Ghisari, M., Bonefeld-Jorgensen, E.C., 2009. Effects of plasticizers and their mixtures on estrogen receptor and thyroid hormone functions. Toxicol. Lett. 189, 67–77.

Ghosh, M.G., Thompson, D.A., Weigel, R.J., 2000. PDZK1 and GREB1 are estrogen-regulated genes expressed in hormone-responsive breast cancer. Cancer Res. 60, 6367–6375.

Hankinson, O., 2008. Why does ARNT2 behave differently from ARNT? Toxicol. Sci. 103, 1–3.

Harrington, W.R., Sheng, S., Barnett, D.H., Petz, L.N., Katzenellenbogen, J.A., Katzenellenbogen, B.S., 2003. Activities of estrogen receptor alpha- and beta-selective ligands at diverse estrogen responsive gene sites mediating transactivation or transrepression. Mol. Cell. Endocrinol. 206, 13–22.

Hatch, E.E., Troisi, R., Wise, L.A., Titus-Ernstoff, L., Hyer, M., Palmer, J.R., Strohsnitter, W.C., Robboy, S.J., Anderson, D., Kaufman, R., Adam, E., Hoover, R.N., 2010. Preterm birth, fetal growth, and age at menarche among women exposed prenatally to diethylstilbestrol (DES). Reprod. Toxicol..

Heldring, N., Pike, A., Andersson, S., Matthews, J., Cheng, G., Hartman, J., Tujague, M., Strom, A., Treuter, E., Warner, M., Gustafsson, J.A., 2007. Estrogen receptors: how do they signal and what are their targets. Physiol. Rev. 87, 905–931.

Hevir, N., Trost, N., Debeljak, N., Rizner, T.L., 2011. Expression of estrogen and progesterone receptors and estrogen metabolizing enzymes in different breast cancer cell lines. Chem. Biol. Interact. 191, 206–216.

Hill, A.J., Heiden, T.C., Heideman, W., Peterson, R.E., 2009. Potential roles of Arnt2 in zebrafish larval development. Zebrafish 6, 79–91.

Hirose, K., Morita, M., Ema, M., Mimura, J., Hamada, H., Fujii, H., Saijo, Y., Gotoh, O., Sogawa, K., Fujii-Kuriyama, Y., 1996. cDNA cloning and tissue-specific expression of a novel basic helix-loop-helix/PAS factor (Arnt2) with close sequence similarity to the aryl hydrocarbon receptor nuclear translocator (Arnt). Mol. Cell. Biol. 16, 1706–1713.

Hosoya, T., Oda, Y., Takahashi, S., Morita, M., Kawauchi, S., Ema, M., Yamamoto, M., Fujii-Kuriyama, Y., 2001. Defective development of secretory neurones in the hypothalamus of Arnt2-knockout mice. Genes Cells 6, 361–374.

Hsu, H.J., Wang, W.D., Hu, C.H., 2001. Ectopic expression of negative ARNT2 factor disrupts fish development. Biochem. Biophys. Res. Commun. 282, 487–492.

Kretzschmar, G., Papke, A., Zierau, O., Moller, F.J., Medjakovic, S., Jungbauer, A., et al., 2010. Estradiol regulates aryl hydrocarbon receptor expression in the rat uterus. Mol. Cell. Endocrinol. 321 (2), 253–257.

Kuiper, G.G., Carlsson, B., Grandien, K., Enmark, E., Haggblad, J., Nilsson, S., Gustafsson, J.A., 1997. Comparison of the ligand binding specificity and transcript tissue distribution of estrogen receptors alpha and beta. Endocrinology 138, 863–870.

Ma, L., 2009. Endocrine disruptors in female reproductive tract development and carcinogenesis. Trends Endocrinol. Metab. 20, 357–363.

Maltepe, E., Keith, B., Arsham, A.M., Brorson, J.R., Simon, M.C., 2000. The role of ARNT2 in tumor angiogenesis and the neural response to hypoxia. Biochem. Biophys. Res. Commun. 273, 231–238.

Martinez, V., Kennedy, S., Doolan, P., Gammell, P., Joyce, H., Kenny, E., Prakash Mehta, J., Ryan, E., O'Connor, R., Crown, J., Clynes, M., O'Driscoll, L., 2008. Drug metabolism-related genes as potential biomarkers: analysis of expression in normal and tumour breast tissue. Breast Cancer Res. Treat. 110, 521–530.

Mitsushima, D., Funabashi, T., Kimura, F., 2003. Estrogen increases messenger RNA and immunoreactivity of aryl-hydrocarbon receptor nuclear translocator 2 in the rat mediobasal hypothalamus. Biochem. Biophys. Res. Commun. 307, 248–253.

Rogers, J.M., Denison, M.S., 2000. Recombinant cell bioassays for endocrine disruptors: development of a stably transfected human ovarian cell line for the detection of estrogenic and anti-estrogenic chemicals. In Vitro Mol. Toxicol. 13, 67–82.

Rogers, J.M., Denison, M.S., 2002. Analysis of the antiestrogenic activity of 2,3,7,8-tetrachlorodibenzo-p-dioxin in human ovarian carcinoma BG-1 cells. Mol. Pharmacol. 61, 1393–1403.

Safe, S., 2004. Endocrine disruptors and human health: is there a problem. Toxicology 205, 3–10.

Scherbakov, A.M., Lobanova, Y.S., Shatskaya, V.A., Krasil'nikov, M.A., 2009. The breast cancer cells response to chronic hypoxia involves the opposite regulation of NF-kB and estrogen receptor signaling. Steroids 74, 535–542.

Schlezinger, J.J., Liu, D., Farago, M., Seldin, D.C., Belguise, K., Sonenshein, G.E., Sherr, D.H., 2006. A role for the aryl hydrocarbon receptor in mammary gland tumorigenesis. Biol. Chem. 387, 1175–1187.

Sekine, H., Mimura, J., Yamamoto, M., Fujii-Kuriyama, Y., 2006. Unique and overlapping transcriptional roles of arylhydrocarbon receptor nuclear translocator (Arnt) and Arnt2 in xenobiotic and hypoxic responses. J. Biol. Chem. 281, 37507–37516.

Sharpe, R.M., Irvine, D.S., 2004. How strong is the evidence of a link between environmental chemicals and adverse effects on human reproductive health? BMJ 328, 447–451.

Sikka, S.C., Wang, R., 2008. Endocrine disruptors and estrogenic effects on male reproductive axis. Asian J. Androl. 10, 134–145.

Swedenborg, E., Pongratz, I., 2010. AhR and ARNT modulate ER signaling. Toxicology 268, 132–138.

Watanabe, M., Yoshida, R., Ueoka, K., Aoki, K., Sasagawa, I., Hasegawa, T., Sueoka, K., Kamatani, N., Yoshimura, Y., Ogata, T., 2007. Haplotype analysis of the estrogen receptor 1 gene in male genital and reproductive abnormalities. Hum. Reprod. 22, 1279–1284.

Welshons, W.V., Thayer, K.A., Judy, B.M., Taylor, J.A., Curran, E.M., vom Saal, F.S., 2003. Large effects from small exposures. I. Mechanisms for endocrine-disrupting chemicals with estrogenic activity. Environ. Health Perspect. 111, 994–1006.

Ziello, J.E., Jovin, I.S., Huang, Y., 2007. Hypoxia-inducible factor (HIF)-1 regulatory pathway and its potential for therapeutic intervention in malignancy and ischemia. Yale J. Biol. Med. 80, 51–60.

In utero exposure to dioxin causes neocortical dysgenesis through the actions of $p27^{Kip1}$

Takayuki Mitsuhashi[a], Junzo Yonemoto[b], Hideko Sone[b], Yasuhiro Kosuge[a,1], Kenjiro Kosaki[a], and Takao Takahashi[a,2]

[a]Department of Pediatrics, School of Medicine, Keio University, Shinjuku-ku, Tokyo 160-8582, Japan; and [b]Research Center for Environmental Risk, National Institute for Environmental Studies, Tsukuba-City, Ibaraki 305-8506, Japan

Edited by Pasko Rakic, Yale University, New Haven, CT, and approved July 13, 2010 (received for review March 8, 2010)

Dioxins have been reported to exert various adverse effects, including cell-cycle dysregulation in vitro and impairment of spatial learning and memory after in utero exposure in rodents. Furthermore, children born to mothers who are exposed to dioxin analogs polychlorinated dibenzofurans or polychlorinated biphenyls have developmental impairments in cognitive functions. Here, we show that in utero exposure to dioxins in mice alters differentiation patterns of neural progenitors and leads to decreased numbers of non-GABAergic neurons and thinner deep neocortical layers. This reduction in number of non-GABAergic neurons is assumed to be caused by accumulation of cyclin-dependent kinase inhibitor $p27^{Kip1}$ in nuclei of neural progenitors. Lending support to this presumption, mice lacking $p27^{Kip1}$ are not susceptible to in utero dioxin exposure. These results show that environmental pollutants may affect neocortical histogenesis through alterations of functions of specific gene(s)/protein(s) (in our case, dioxins), exerting adverse effects by altering functions of $p27^{Kip1}$.

environmental pollutants | cerebral cortex | development | neuronal progenitor cells | cell cycle

Dioxins are ubiquitous environmental pollutants that have been known to disturb hormonal homeostasis in mammals (1–3). In utero exposure to 2,3,7,8-tetrachlorodibenzo-*p*-dioxin (TCDD), one of the most potent dioxins, has been shown to cause impaired spatial learning and memory in rats (4). Furthermore, in humans, it is reported that children born to mothers who are exposed to dioxin analogs polychlorinated dibenzofurans (PCDFs) or polychlorinated biphenyls (PCBs) have developmental impairments in higher cognitive functions (2, 5). Additionally, a recent report describes the relationship between prenatal exposure level of polycyclic aromatic hydrocarbons and child intelligence at 5 y of age (6). However, the mechanisms by which dioxin exposure in utero affects the higher cortical functions after birth remain undetermined.

Non-GABAergic projection neurons, accounting for 80% of the neocortical neurons, are produced by proliferation/differentiation of neuronal progenitor cells (NPCs) constituting the pseudostratified ventricular epithelium [PVE; roughly coexistent with the ventricular zone (VZ)] along the lateral ventricular surface of the embryonic forebrain. The term PVE has been adopted, because it excludes postmitotic, premigratory neuroblasts of the subventricular zone (7, 8). In mice, the NPCs undergo 11 cell divisions during the period of neocortical histogenesis, with the length of the cell cycle (T_C) increasing by 2-fold from 8 to 18 h, mainly because of prolongation of the G1 phase of the cell cycle (T_{G1}) (8). During the same period, the proportion of daughter cells that become postmitotic during each cell cycle [quiescent (Q) fraction] increases (9). It is of critical importance that the layer position of the non-GABAergic projection neurons is strongly correlated with the cell cycle of origin (that is, the cell cycle at which a given non-GABAergic neuron becomes mitotically quiescent and starts radial migration to the neocortex) (10). Taken together, the regulated patterns of increase of the T_{G1} and Q fractions and strict correlation between the layer position and the cell cycle of origin both strongly suggest a link between cell-cycle regulation of the G1 phase and neuronal cell-class determination (layer destination of projection neurons) (10).

Progression of the cell cycle is precisely controlled by a set of proteins including cyclins, cyclin dependent kinases (CDKs), and CDK inhibitors (11). $p27^{Kip1}$, one of the CDK inhibitors, specifically inhibits the activity of cyclin E/CDK2 kinase and inhibits entry of the cells into the S phase (12, 13). Indeed, some of the critical events during the G1 phase of the cell cycle in NPCs are regulated by $p27^{Kip1}$: alterations in $p27^{Kip1}$ expression in the NPCs result in changes in the Q fraction, thereby altering the number of neurons to be produced and hence, the thickness of the neocortex. Specifically, overexpression of $p27^{Kip1}$ in NPCs in vivo increases the Q fraction (that is, promotes differentiation of the NPCs), with a resultant thinner neocortex (14, 15), whereas the lack of $p27^{Kip1}$ decreases the Q fraction, resulting in a thicker neocortex (16). It is worthy of note in this context that TCDD has been reported to induce $p27^{Kip1}$ and delay the G1 phase of the cell cycle in a hepatoma cell line, fetal thymocytes, and human neuronal cell line (17). Taken together, these observations suggest that in utero exposure to TCDD is likely to alter the proliferative behaviors of the NPCs by inducing $p27^{Kip1}$ protein expression, resulting in abnormalities of neocortical histogenesis.

Here, we report that in utero exposure to TCDD indeed modified the $p27^{Kip1}$ activities in NPCs to cause neocortical dysgenesis. These observations can be explained by a hypothetical mathematical model where both the increase in Q fraction and the neuronal class switch occur prematurely compared with that under physiological conditions.

Results

TCDD Exposure in Utero Reduced the Size of the Telencephalon and Thickness of the Neocortex as Assessed on Postnatal Day 21. The telencephalon, olfactory bulb, and cerebellum of TCDD-treated mice showed a normal appearance on postnatal day (P) 21 (Fig. 1*A*). However, the forebrains in these TCDD-treated animals were smaller, with the width and length being reduced by 4.78% (9.48 ± 0.063 mm vs. 9.93 ± 0.030 mm in the controls; $P < 0.001$, $n = 10$) and 2.29% (8.37 ± 0.048 vs. 8.57 ± 0.035 mm; $P = 0.004$, $n = 10$), respectively, compared with the values in the controls. The reductions in the width and length of the telencephalon indicate that TCDD exposure in utero caused roughly 7% reduction of the neocortical surface area. The thickness of the primary somatosensory cortex was reduced by 14.9% (750 ± 29.2 vs. 881.3 ± 13.2 μm; $P < 0.001$, $n = 6$) (Fig. 1*B*); the thickness of the deeper

Author contributions: T.M., J.Y., H.S., K.K., and T.T. designed research; T.M. and Y.K. performed research; T.M. and T.T. analyzed data; and T.M. and T.T. wrote the paper.

The authors declare no conflict of interest.

This article is a PNAS Direct Submission.

Freely available online through the PNAS open access option.

[1]Present address: Research Unit of Pharmacology, School of Pharmacy, Nihon University, Chiba 274-8555, Japan.

[2]To whom correspondence should be addressed. E-mail: ttakahashi@z3.keio.jp.

This article contains supporting information online at www.pnas.org/lookup/suppl/doi:10.1073/pnas.1002960107/-/DCSupplemental.

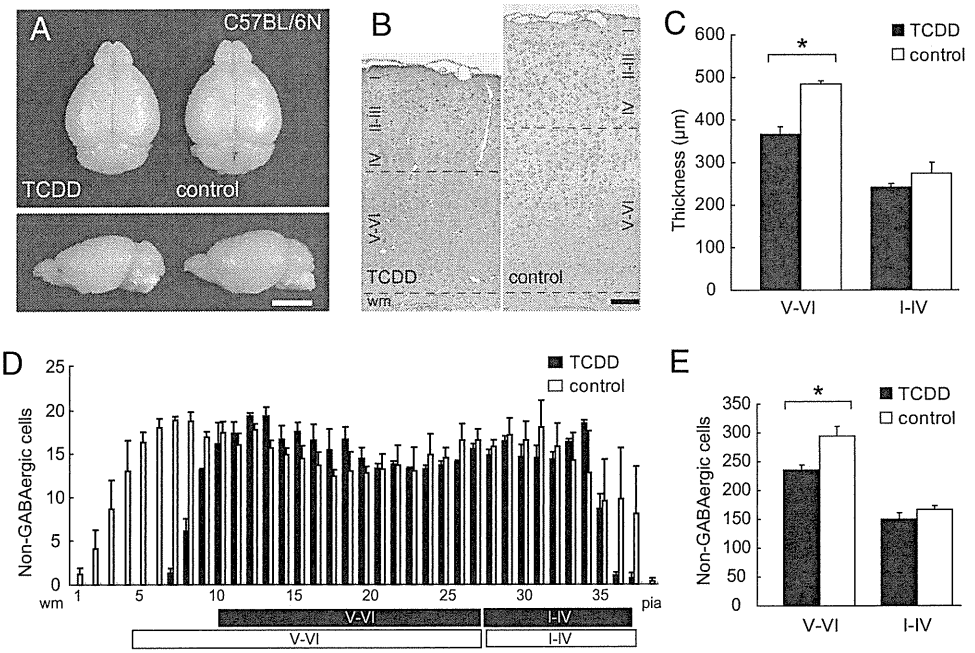

Fig. 1. Effects of in utero TCDD exposure observed on postnatal day 21. (*A*) Macroscopic dorsal and lateral overview of the whole brain from TCDD-treated and control C57BL/6N mice. (Scale bar, 5 mm.) (*B*) High-power view of the primary somatosensory neocortex of the TCDD-treated and control mice. Brown cells, GABA-positive interneurons; purple nuclei, either non-GABAergic projection neurons or glial cells; black dotted lines, boundaries between layers I-IV/V-VI and gray matter/white matter (wm). (Scale bar, 100 μm.) (*C*) Thickness of layers V-VI and I-IV in the TCDD-treated and control mice shown in *B*. (*D*) Numbers of non-GABAergic neurons counted in each bin (250 μm in width and 25 μm in height) lined serially from wm to the pial surface (pia) in the primary somatosensory neocortex shown in *B*. Black and white boxes under the abscissa indicate layers I-IV/V-VI in the neocortex of the TCDD-treated and control mice, respectively. (*E*) Total number of non-GABAergic neurons in layers V-VI and I-IV. $*P < 0.05$. Error bars in *C–E*, SEM.

cortical layers (layers V-VI) was reduced by 24.1% (366.7 ± 16.67 vs. 483.3 ± 8.33 μm; $P = 0.005, n = 6$), whereas no significant change in the thickness of the superficial layers (layers I-IV) was noted (241.7 ± 8.33 vs. 275.0 ± 25.0 μm; $P = 0.38, n = 6$) (Fig. 1*C*).

TCDD Exposure in Utero Reduced the Number of Non-GABAergic Neurons in the Deeper Cortical Layers as Assessed on Postnatal Day 21. We identified non-GABAergic projection neurons by the lack of positive immunohistochemical staining of the cells with anti-GABA antibody (Fig. 1 *B* and *D*). The number of non-GABAergic projection neurons in the primary somatosensory neocortex on P21 was significantly reduced in the deeper layers of the TCDD-treated animals by 20.0% compared with that in normal controls (Fig. 1*E*) (235.6 ± 9.24 vs. 294.3 ± 16.9 per 1,000 μm^2; $P = 0.037, n = 3$). However, there was no significant difference in the number of non-GABAergic neurons in the superficial layers of the cortex in the TCDD-treated animals compared with that in the controls (Fig. 1*E*) (149.8 ± 10.9 vs. 166.8 ± 6.14 per 1,000 μm^2; $P = 0.246, n = 3$). No alteration in the cell-packing density of the non-GABAergic projection neurons was observed in either the deeper or superficial layers in the TCDD-treated animals. Taken together, we concluded that the reduction in neocortical thickness of the TCDD-treated mice was caused by the reduction in the number of non-GABAergic projection neurons in the deeper cortical layers.

Total Cell Cycle Length of the NPCs Was Not Altered by TCDD Exposure in Utero. Next, we examined the TCDD-treated embryonic forebrains on E12, the time point at which the non-GABAergic neurons of the deeper layers (layers V–VI) are to be produced (10). Histologically, the dorsomedial cerebral wall, the future primary somatosensory neocortex, was normal in the TCDD-treated embryos (Fig. 2*A*). The S phase zone, where accumulation of the nuclei of the NPCs is observed during the S phase of the cell cycle, in the dorsomedial cerebral wall was located between 60 and 70 μm from the lateral ventricular border on E12 in the TCDD-treated mice, similar to the finding in the normal control mice (Fig. 2 *A* and *B*) ($n = 4$). At 4 h after exposure to bromodeoxyuridine (BrdU), BrdU-positive nuclei moved to the ventricular surface in both the TCDD-treated and control animals, indicating that the interkinetic nuclear migration in the embryonic forebrain operated normally in the TCDD-treated mice (Fig. 2*C*) ($n = 3$). After 6.5 h exposure to BrdU, virtually all of the nuclei in the VZ were BrdU-positive in both the TCDD-treated and control mice, indicating that the growth fractions in the VZ were nearly equal to 1.0 in both the TCDD-treated and control mice (Fig. 2*D*) ($n = 3$). The results of cumulative BrdU labeling (Fig. 2*E*) (18) revealed that the total cell-cycle length of the NPCs in the forebrain of the TCDD-treated animals was 10.7 h, not significantly different from that in the controls (Table 1).

TCDD Exposure in Utero Promoted Early Cell Cycle Exit of NPCs. We then identified the NPCs in the Q fraction and P fraction (the fraction of daughter cells that remain proliferative; $P = 1.0 - Q$) on E12 by using two S-phase tracers, iododeoxyuridine (IdU) and BrdU (Fig. 2*F*) (15, 19). In the dorsomedial cerebral wall of the TCDD-treated mice, the IdU-positive nuclei (blue nuclei) were located in the outer margin of the S-phase zone in both the P + Q and Q experiments (Fig. 2*F*). The distribution patterns of the P + Q and Q cells were not different between the TCDD-treated and control animals (Fig. 2*G*). An increase in the number of Q cells was observed in the TCDD-treated animals, with an estimated Q fraction of 0.17, which represented a 21.4% increase compared with the value in the controls (Table 2) ($n = 3$).

TCDD Exposure in Utero Increased the Nuclear Fraction of the $p27^{Kip1}$ Protein in the NPCs. To elucidate the molecular mechanisms underlying the aforementioned changes, we first investigated the TCDD-induced changes in the mRNA expression levels of cell-cycle regulatory genes in the dorsomedial cerebral wall by dot blot hybridization (Fig. 3 *A* and *B*) ($n = 5$). We observed up-regulation

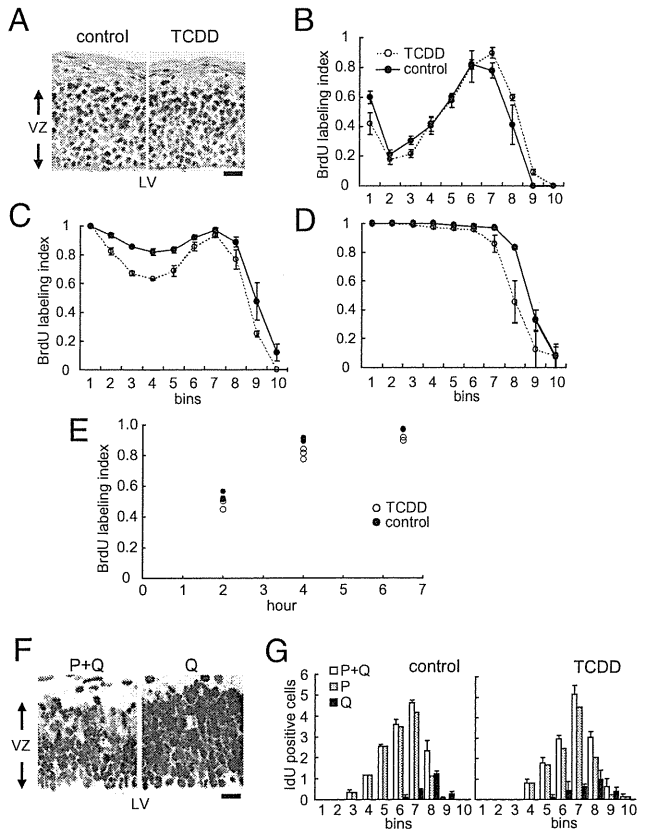

Fig. 2. Effects of in utero TCDD exposure on the cell-cycle kinetics of the NPCs. (*A*) High-power views of the dorsomedial cerebral wall of the E12 forebrains of the control and TCDD-treated mice. Black, BrdU-labeled nuclei; red, non–BrdU-labeled nuclei; VZ, ventricular zone; LV, lateral ventricle. (Scale bar, 10 μm.) (*B*) The 2-h BrdU-labeling index was evaluated in each bin (100 μm in width and 10 μm in height) lined serially from the lateral ventricle to the pial surface in the ventricular zone. The 4-h (*C*) and 6.5-h (*D*) BrdU-labeling indices are also shown. (*E*) Total labeling indices after cumulative BrdU exposure. (*F*) High-power views of the dorsomedial area of the E12 forebrains of mice exposed to TCDD. Blue nuclei, IdU-only positive; brown nuclei, double positive for IdU and BrdU. In the P + Q experiment (*Left*), blue nuclei correspond to the P + Q fraction cells. In the Q experiment (*Right*), blue cells correspond to only the Q fraction cells. (Scale bar, 10 μm.) (*G*) The number of Q fraction cells and P + Q fraction cells that were counted in each bin in control (*Left*) and TCDD-treated embryos (*Right*).

of the *p27*^{Kip1} and *p15*^{INK4b} mRNAs in the E12 forebrain in the TCDD-treated animals compared with the expressions in the controls (Fig. 3*B*): both *p27*^{Kip1} and *p15*^{INK4b} are CDK inhibitors that are known to promote exit from the cell cycle (11). We then analyzed the p27^{Kip1} and p15^{INK4b} protein levels by immunoblot analysis of lysates of the E12 dorsomedial cerebral walls. The p27^{Kip1} and p15^{INK4b} protein levels in the total tissue lysate were not significantly different between the TCDD-treated and control animals. However, when only the nuclear fractions from the dorsomedial cerebral wall were analyzed, the p27^{Kip1} protein level was

Table 1. Lengths of each phase of the cell cycle estimated by cumulative BrdU labeling index

	$T_C - T_S$	T_C	T_S	T_{G1}	T_{G2+M}
TCDD	7.0	10.7	3.7	5.0	2.0
Control	6.3	10.5	4.3	4.3	2.0

T_C, length of the total cell cycle; T_S, length of S phase, T_{G1}, length of G1 phase; T_{G2+M}, length of G2 + M phase.

Table 2. Q fraction analysis

	N_{P+Q}	N_Q	P fraction	Q fraction
TCDD	14.5	2.6	0.82	0.17
Control	14.7	2.1	0.86	0.14

N_{P+Q}, number of blue nuclei in the P + Q experiment; N_Q, number of blue nuclei in the Q experiment; Q fraction, N_Q/N_{P+Q}; P fraction, 1 – Q.

about 2.5-fold higher in the TCDD-treated mice compared with the levels in the controls, the difference being significant (Fig. 3 *C* and *D*) ($n = 4$).

TCDD Exposure in Utero Did Not Reduce the Number of Non-GABAergic Neurons in the Deeper Cortical Layers of the p27^{Kip1} Knockout Mice. To further confirm the role of p27^{Kip1} in the events associated with TCDD exposure in utero, we repeated the in utero TCDD exposure experiments using p27^{Kip1} knockout mice (p27$^{-/-}$) (Fig. 4*A*) (20–22). We have previously reported that an increased thickness of the somatosensory neocortex on P21 in p27$^{-/-}$ mice compared with that in the wild-type animals is caused by the overproduction of non-GABAergic projection neurons destined for the superficial neocortical layers (16). Here, neither the layer thickness nor the number in non-GABAergic neurons of the primary somatosensory neocortex on P21 was significantly reduced in the TCDD-treated p27$^{-/-}$ compared with the findings in the controls (i.e., p27$^{-/-}$ mice exposed to corn oil; $n = 5$) (Fig. 4 *B–D*).

Discussion

Reduction in the Peak Population Size of NPCs by TCDD Exposure. The neocortical surface area, although influenced by multiple factors such as neuropil expansion and other growth-related parameters, is mostly determined during its ontogeny by the degree of tangential expansion of PVE (9). The size of the PVE, in turn, is virtually exclusively determined by the maximum population size of the NPCs, because dominant constituents of the PVE are the NPCs (9). Thus, the reduction of the neocortical surface area in the TCDD-treated mice (Fig. 1) strongly indicates a decrease in the maximum number of NPCs during neocortical histogenesis. The population size of the NPCs is governed solely by the pattern of ascent of the Q fraction during the early phase of neocortical histogenesis, and the maximum size is reached at the

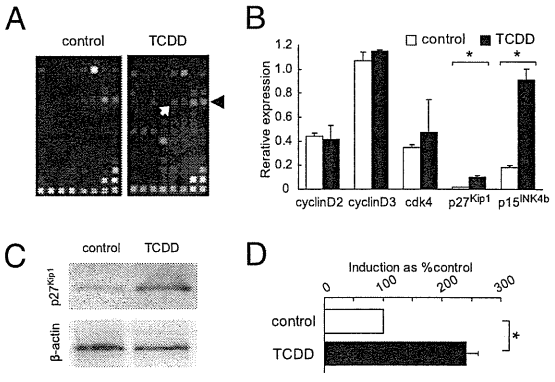

Fig. 3. Effects of in utero TCDD exposure on the expression profile of cell-cycle regulatory genes in the NPCs. (*A*) cDNA expression arrays hybridized with biotinylated probes generated from the embryonic forebrain of control and TCDD-treated mice. Black arrowhead and white arrow indicate signals from *p15*^{INK4b} and *p27*^{Kip1}, respectively. (*B*) mRNA expression after TCDD exposure. The β-actin signal equals 1.0. (*C*) Immunoblot analysis of nuclear p27^{Kip1} protein in the forebrains of the embryos of the control and TCDD-treated mice. β-actin levels were used to verify equal loading of the samples. (*D*) TCDD-induced increase of nuclear p27^{Kip1} protein. Bars, percentage signal intensity relative to the levels in the control embryos set at 100%. *$P < 0.05$. Error bars in *B* and *D*, SEM.

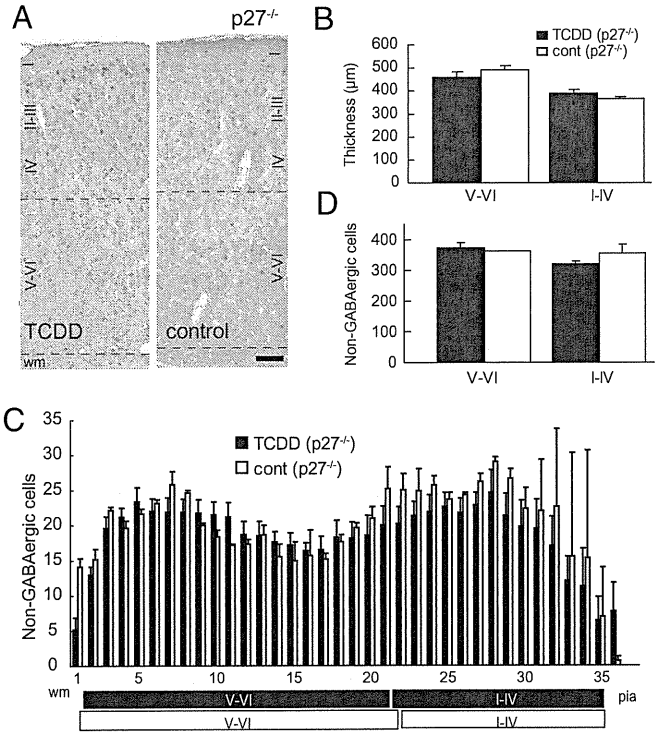

Fig. 4. Effects of in utero TCDD exposure in $p27^{Kip1}$ knockout mice as assessed on P21. (*A*) High-power view of the primary somatosensory neocortex of $p27^{Kip1}$ knockout mice ($p27^{-/-}$) exposed to TCDD and control mice. Brown cells, GABA-positive interneurons; purple nuclei, either non-GABAergic projection neurons or glial cells; black dotted lines, boundaries between layers I-IV/V-VI and gray matter/wm. (Scale bar, 100 μm.) (*B*) Thickness of layers V-VI and I-IV in the TCDD-treated and control mice shown in *A*. (*C*) Numbers of non-GABAergic neurons counted in each bin (250 μm in width and 25 μm in height) lined serially from the wm to the pia in the primary somatosensory neocortex shown in *A*. Black and white boxes under the abscissa indicate layers I-IV/V-VI in the neocortex of the TCDD-treated and control mice, respectively. (*D*) Total number of non-GABAergic neurons in layers V-VI and I-IV. Error bars in *B–D*, SEM.

point where the Q fraction reaches 0.5: the earlier the Q fraction reaches 0.5, the smaller the peak NPC population size (9, 23). Because no increase in apoptosis was noted in the PVE of the TCDD-treated mice, we conclude that TCDD exposure in utero reduced the peak population size of the NPCs by inducing a premature increase of the Q fraction. Because the degree of surface-area reduction is relatively small (7%), the premature increase in the Q fraction to 0.5 was likely to have occurred relatively late during the period, when the Q fraction was between 0 and 0.5. This assumption agrees with the previously reported $p27^{Kip1}$ expression pattern among NPCs (that is, extremely low at the outset with the peak expression in the middle of neuronogenesis) (24).

Possible Mechanisms of Underproduction of Non-GABAergic Neurons in the Deeper Cortical Layers. It is of critical importance to note that only those projection neurons that are produced during the early phase of neuronogenesis when the Q fraction is less than 0.5 become destined for the deeper cortical layers (9, 10). It follows that the time point at which the Q fraction reaches 0.5 during neuronogenesis is the critical time window for the phenotypic switch from the deep- to superficial-layer neurons (25). Taken together, we conclude that the abnormal increase of the Q fraction during the early phase of neuronogenesis induced by TCDD exposure leads not only to a decrease of the peak population size of the NPCs but also to premature-cell phenotype switch and consequently, a decrease in the number of non-GABAergic projection neurons in the deeper cortical layers.

Of note, the progenitor population of the PVE is already committed to their lineage without pluripotency. In fact, our preliminary results indicated that GABAergic neurons and glial cells were also reduced in number, and such reduction was not observed in $p27^{-/-}$. It follows that $p27^{Kip1}$ is likely to be responsible for determining the size of those neural populations as well. The proliferation/differentiation characteristics of progenitor populations of GABAergic neurons (NPCs of the ganglionic eminence) and glial cells surely deserve further investigation (26).

Mechanism of Nuclear Accumulation of $p27^{Kip1}$ After TCDD Exposure. The premature increase of the Q fraction, as described in the foregoing paragraphs, is the underlying biological mechanism for the TCDD-induced abnormality of neocortical histogenesis. The increase of the Q fraction seems to be attributable to the nuclear accumulation of $p27^{Kip1}$: this hypothesis is lent strong support by the finding that mice lacking the $p27^{Kip1}$ protein showed almost no alteration of the neocortical thickness after TCDD exposure (Fig. 4). Thus, $p27^{Kip1}$ may be involved in the cascade of critical events anywhere downstream of the direct effect of TCDD. There has been no report to this date, to the best of our knowledge, on the effect of TCDD on the subcellular localization of the $p27^{Kip1}$. The nuclear fraction of $p27^{Kip1}$ protein is determined by the balance of the protein transportation into and out of the nuclei. However, the expression levels of Jab-1, Akt, and Skp2 proteins, known to be involved in the nuclear transportation and degradation of the $p27^{Kip1}$ protein, were not found to be altered in the NPCs of the TCDD-treated mice (27–31). Another intriguing observation is the stability of the total cell-cycle length observed, despite TCDD exposure (Table 1). The stabilizing mechanisms of the cell-cycle kinetics shown in *Drosophila melanogaster* (32) may also be involved in the homeostasis of the NPC cell cycle after in utero TCDD exposure.

This report quantitatively evaluates the effects of an environmental pollutant on neocortical histogenesis. In addition, this study is an example of an experimental model where the phenotypic severity of a particular adverse effect of a given environmental substance was found to be dependent on the genotype of the animals, which has profound implications from the viewpoint of toxicogenomics (33). Furthermore, our mathematical model of neocortical histogenesis has been shown to be a powerful tool to examine neocortical dysgenesis after relatively subtle alterations in the decision-making characteristics of the NPCs. We believe that this analytical method would be applicable to various environmental substances that may have adverse effects on human CNS development.

Materials and Methods

TCDD Administration. TCDD (Cambridge Isotope Laboratory) was dissolved in corn oil at a concentration of 2 μg mL^{-1}. A single dose of TCDD solution, or corn oil {0.01 mL [gram body weight (g bw)]$^{-1}$} as control, was administered orally to pregnant C57BL/6N and $p27^{-/-}$ mice on E7 using a disposable feeding needle. The total dose of TCDD administered was 20 μg (kg bw)$^{-1}$. This dose was adopted, because it was expected not to affect the mother in terms of child-rearing behavior. In fact, no adverse effect was observed during pregnancy and the postpartum period.

Measurement of the Dimensions of the Telencephalon. Brains from either TCDD- or corn oil-exposed mice on P21 were fixed in 4% phosphate-buffered formaldehyde containing 0.5% glutaraldehyde by transcardiac perfusion. The length and width of 10 telencephalons obtained from either TCDD- or corn oil-exposed P21 mice embryos were measured with micrometer calipers.

GABA Immunohistochemistry, Cumulative BrdU Labeling Analysis, and Q Fraction Analysis. GABA immunohistochemistry was performed as described previously using anti-GABA antibody (Chemicon International) (16). Cumulative BrdU labeling analysis (18) and Q fraction analysis (9, 15, 34) were performed as previously described. Detailed methods are described in *SI Materials and Methods*.

mRNA Expression Analysis and Immunoblot Analysis. Total RNA was isolated from E12 cerebral walls using the RNeasy Protect kit (Qiagen), and the mRNA was purified using the MicroPolyA Pure kit (Ambion) for generating biotinylated cDNA probes. The biotinylated probes were hybridized to cDNA expression arrays (GE array Q series Mouse Cell Cycle Gene Array; Superarray). Immunoblot analyses were conducted using anti-$p27^{Kip1}$, $p15^{INK4b}$, cyclin E, Skp2, β-actin (Santa Cruz Biotechnology), cyclin D1, CDK2, CDK4 (Sigma), AKT (Cell Signaling Technology), and Jab-1 (GeneTex) antibodies. Detailed methods are described in *SI Materials and Methods*.

ACKNOWLEDGMENTS. $p27^{Kip1}$ knockout mice were provided by Nippon Roche K.K. which were generated by Nakayama K, et al. (20). We acknowledge the assistance of Ms. H. Zaha and the discussions that we held with Drs. C. Tohyama and T. Goto during the preparation of this manuscript. This work was supported by Grant-in-Aid for Young Scientists (B) of the Ministry of Education, Culture, Sports, Science and Technology of Japan (17790723, 20790744, and 22791001 to T.M.) and Grant-in-Aid for Scientific Research (B) of Japan Society for the Promotion of Science (JSPS) (15390327, 18390302, and 20390299 to T.T.) and the 21st century Center of Excellence program of JSPS.

1. Barsotti DA, Abrahamson LJ, Allen JR (1979) Hormonal alterations in female rhesus monkeys fed a diet containing 2,3,7,8-tetrachlorodibenzo-p-dioxin. *Bull Environ Contam Toxicol* 21:463–469.
2. Birnbaum LS (1994) Endocrine effects of prenatal exposure to PCBs, dioxins, and other xenobiotics: Implications for policy and future research. *Environ Health Perspect* 102: 676–679.
3. Poland A, Knutson JC (1982) 2,3,7,8-tetrachlorodibenzo-p-dioxin and related halogenated aromatic hydrocarbons: Examination of the mechanism of toxicity. *Annu Rev Pharmacol Toxicol* 22:517–554.
4. Markowski VP, Cox C, Preston R, Weiss B (2002) Impaired cued delayed alternation behavior in adult rat offspring following exposure to 2,3,7,8-tetrachlorodibenzo-p-dioxin on gestation day 15. *Neurotoxicol Teratol* 24:209–218.
5. Chen YC, Guo YL, Hsu CC, Rogan WJ (1992) Cognitive development of Yu-Cheng ("oil disease") children prenatally exposed to heat-degraded PCBs. *JAMA* 268:3213–3218.
6. Perera FP, et al. (2009) Prenatal airborne polycyclic aromatic hydrocarbon exposure and child IQ at age 5 years. *Pediatrics* 124:e195–e202.
7. Sauer FC (1935) Mitosis in the neural tube. *J Comp Neurol* 62:377–405.
8. Takahashi T, Nowakowski RS, Caviness VS, Jr (1995) The cell cycle of the pseudostratified ventricular epithelium of the embryonic murine cerebral wall. *J Neurosci* 15:6046–6057.
9. Takahashi T, Nowakowski RS, Caviness VS, Jr (1996) The leaving or Q fraction of the murine cerebral proliferative epithelium: a general model of neocortical neuronogenesis. *J Neurosci* 16:6183–6196.
10. Takahashi T, Goto T, Miyama S, Nowakowski RS, Caviness VS, Jr (1999) Sequence of neuron origin and neocortical laminar fate: Relation to cell cycle of origin in the developing murine cerebral wall. *J Neurosci* 19:10357–10371.
11. Sherr CJ, Roberts JM (1999) CDK inhibitors: Positive and negative regulators of G1-phase progression. *Genes Dev* 13:1501–1512.
12. Toyoshima H, Hunter T (1994) p27, a novel inhibitor of G1 cyclin-Cdk protein kinase activity, is related to p21. *Cell* 78:67–74.
13. Polyak K, et al. (1994) Cloning of p27Kip1, a cyclin-dependent kinase inhibitor and a potential mediator of extracellular antimitogenic signals. *Cell* 78:59–66.
14. Mitsuhashi T, et al. (2001) Overexpression of p27Kip1 lengthens the G1 phase in a mouse model that targets inducible gene expression to central nervous system progenitor cells. *Proc Natl Acad Sci USA* 98:6435–6440.
15. Tarui T, et al. (2005) Overexpression of p27 Kip 1, probability of cell cycle exit, and laminar destination of neocortical neurons. *Cereb Cortex* 15:1343–1355.
16. Goto T, Mitsuhashi T, Takahashi T (2004) Altered patterns of neuron production in the p27 knockout mouse. *Dev Neurosci* 26:208–217.
17. Kolluri SK, Weiss C, Koff A, Göttlicher M (1999) p27(Kip1) induction and inhibition of proliferation by the intracellular Ah receptor in developing thymus and hepatoma cells. *Genes Dev* 13:1742–1753.
18. Takahashi T, Nowakowski RS, Caviness VS, Jr (1992) BUdR as an S-phase marker for quantitative studies of cytokinetic behaviour in the murine cerebral ventricular zone. *J Neurocytol* 21:185–197.
19. Nowakowski RS, Lewin SB, Miller MW (1989) Bromodeoxyuridine immunohistochemical determination of the lengths of the cell cycle and the DNA-synthetic phase for an anatomically defined population. *J Neurocytol* 18:311–318.
20. Nakayama K, et al. (1996) Mice lacking p27(Kip1) display increased body size, multiple organ hyperplasia, retinal dysplasia, and pituitary tumors. *Cell* 85:707–720.
21. Kiyokawa H, et al. (1996) Enhanced growth of mice lacking the cyclin-dependent kinase inhibitor function of p27(Kip1). *Cell* 85:721–732.
22. Fero ML, et al. (1996) A syndrome of multiorgan hyperplasia with features of gigantism, tumorigenesis, and female sterility in p27(Kip1)-deficient mice. *Cell* 85: 733–744.
23. Takahashi T, Nowakowski RS, Caviness VS, Jr (1997) The mathematics of neocortical neuronogenesis. *Dev Neurosci* 19:17–22.
24. Delalle I, Takahashi T, Nowakowski RS, Tsai LH, Caviness VS, Jr (1999) Cyclin E-p27 opposition and regulation of the G1 phase of the cell cycle in the murine neocortical PVE: A quantitative analysis of mRNA in situ hybridization. *Cereb Cortex* 9:824–832.
25. Caviness VS, Jr, et al. (2003) Cell output, cell cycle duration and neuronal specification: A model of integrated mechanisms of the neocortical proliferative process. *Cereb Cortex* 13:592–598.
26. Bhide PG (1996) Cell cycle kinetics in the embryonic mouse corpus striatum. *J Comp Neurol* 374:506–522.
27. Tomoda K, et al. (2002) The cytoplasmic shuttling and subsequent degradation of p27Kip1 mediated by Jab1/CSN5 and the COP9 signalosome complex. *J Biol Chem* 277: 2302–2310.
28. Kossatz U, et al. (2004) Skp2-dependent degradation of p27kip1 is essential for cell cycle progression. *Genes Dev* 18:2602–2607.
29. Carrano AC, Eytan E, Hershko A, Pagano M (1999) SKP2 is required for ubiquitin-mediated degradation of the CDK inhibitor p27. *Nat Cell Biol* 1:193–199.
30. Nakayama K, et al. (2000) Targeted disruption of Skp2 results in accumulation of cyclin E and p27(Kip1), polyploidy and centrosome overduplication. *EMBO J* 19:2069–2081.
31. Liang J, et al. (2002) PKB/Akt phosphorylates p27, impairs nuclear import of p27 and opposes p27-mediated G1 arrest. *Nat Med* 8:1153–1160.
32. Reis T, Edgar BA (2004) Negative regulation of dE2F1 by cyclin-dependent kinases controls cell cycle timing. *Cell* 117:253–264.
33. Shih DM, et al. (1998) Mice lacking serum paraoxonase are susceptible to organophosphate toxicity and atherosclerosis. *Nature* 394:284–287.
34. Hayes NL, Nowakowski RS (2000) Exploiting the dynamics of S-phase tracers in developing brain: Interkinetic nuclear migration for cells entering versus leaving the S-phase. *Dev Neurosci* 22:44–55.

Review

Oxygenomics in environmental stress

H. Sone[1], H. Akanuma[1], T. Fukuda[2]

[1]*National Institute for Environmental Studies, Tsukuba, Ibaraki, Japan*
[2]*Tohoku University, Aoba-ku, Sendai, Japan*

Environmental stressors such as chemicals and physical agents induce various oxidative stresses and affect human health. To elucidate their underlying mechanisms, etiology and risk, analyses of gene expression signatures in environmental stress-induced human diseases, including neuronal disorders, cancer and diabetes, are crucially important. Recent studies have clarified oxidative stress-induced signaling pathways in human and experimental animals. These pathways are classifiable into several categories: reactive oxygen species (ROS) metabolism and antioxidant defenses, p53 pathway signaling, nitric oxide (NO) signaling pathway, hypoxia signaling, transforming growth factor (TGF)-β bone morphogenetic protein (BMP) signaling, tumor necrosis factor (TNF) ligand–receptor signaling, and mitochondrial function. This review describes the gene expression signatures through which environmental stressors induce oxidative stress and regulate signal transduction pathways in rodent and human tissues.

Keywords: Oxygenomics, environmental stress, gene expression signatures, signal transduction pathways

Introduction

Oxidative stress in the form of excess reactive oxygen species (ROS) or reactive nitrogen species (RNS) can affect cells deleteriously or beneficially. Such stress might be generated by intracellular or extracellular sources. Furthermore, oxidative stress can cause various human diseases. Environmental stress is a key contributor to human disease. Myriad substances such as metals, particulate materials, smoke, pesticides, and physical agents are environmental stressors (see Table 1) that contribute to many diseases. Concerns related to environmental stressor-related diseases such as cancer, chronic lung disease, diabetes mellitus, neurodegenerative diseases, and reproductive disorders have been raised recently. Research efforts elucidating the modes by which environmental stressors influence the development and progression of diseases or exploring preventive approaches are expected to engender further improvements in our knowledge. Understanding environmental stressor-induced influences at the molecular level will also provide a wealth of information related to the exploration of biomarkers for environmental stressor-related diseases.[1–3]

The mechanisms of redox adaptation in living bodies and cells might involve multiple influences on an active redox-sensitive signaling pathway, such as ROS metabolism and antioxidant defenses, p53 pathway signaling, nitric oxide (NO) signaling pathway, hypoxia signaling, transforming growth factor (TGF)-β-bone morphogenetic protein (BMP) signaling, tumor necrosis factor (TNF) ligand–receptor signaling, and mitochondrial function (Table 2). For example, transcription factors such as nuclear factor-κB (NF-κB), nuclear factor erythroid 2-related factor 2 (Nrf2), c-Jun and hypoxia-inducible factor-1 (HIF-1) engender increased expression of anti-oxidant molecules such as superoxide dismutase (SOD), catalase, thioredoxin, and the GSH antioxidant system. Metal ions such as arsenic(III/V)

Correspondence to: Correspondence to: Dr Hideko Sone, National Institute for Environmental Studies, 16-2 Onogawa, Tsukuba, Ibaraki, Japan
E-mail: hsone@nies.go.jp
Received 12 December 2009, manuscript accepted 9 April 2010

DOI 10.1179/174329210X12650506623843

Table 1 Environmental stressors that induce oxidative stress

Sources	
Metals	Antimony (Sb), arsenic (As), beryllium (Be), cadmium (Cd), chromium (Cr), cobalt (Co), copper (Cu), lead (Pb), mercury (Hg), nickel (Ni), vanadium (V)
Particulate matter and smoke	PM10, PM2.5, carbon monoxide (CO) sulfur dioxide (SO_2), nitrogen oxides (NOx), ozone (O_3), asbestos
Agriculture-related chemicals	Pesticides, fungicides
Persistent organic pollutants	Aldrin, chlordane, DDT, dieldrin, endrin, heptachlor, hexachlorobenzene, mirex, polychlorinated biphenyls, polychlorinated dibenzo-*p*-dioxins, polychlorinated dibenzofurans, toxaphene, carcinogenic polycyclic aromatic hydrocarbons, certain brominated flame-retardants, organometallic compounds such as tributylin TBT
Hormones and environmental hormones (endocrine disrupting chemicals)	Estradiol, dehydrotestosterone, bisphenols, phthalates
Physical agents	Burn Radiation UV radiation

or copper(II) directly influence expression levels of those transcription factors and induce various oxidative stress events including thiol molecule perturbation, generation of oxidative DNA adducts, and induction of oxidative molecular biomarkers.[4–7] Non-metal chemicals such as retinoic acids and 2,3,7,8-tetrachlorodibenzo-*p*-dioxin (TCDD) are also known to influence the expression of oxidative stress-related genes and proteins during carcinogenesis and during embryonic development.[8–11] In relation to cancer, a growing tumor might also produce intracellular and extracellular oxidative stress, which can modify its malignant features. Endogenous sources of tumor ROS or RNS include impaired intracellular genomes or proteomes, metabolism pathways, and xenobiotic metabolism. Consequently, the study of transcriptional regulation of gene expression in the research field of oxidative stress has been useful for identifying new *trans*-regulatory factors or new biomarkers induced by exposure to environmental stressors.

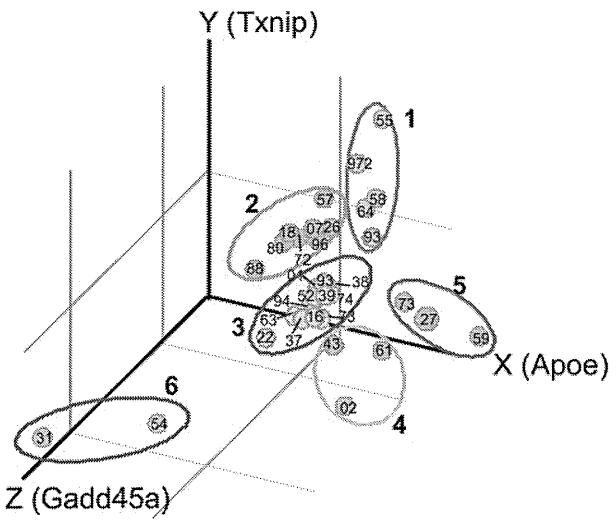

Figure 1 Principal component analysis of oxidative stress-induced genes extracted from 33 independent datasets in GEO. Numbers indicate the last two or three digits of GEOID

Microarray technology has been used in environmental toxicology and biology studies and has led to the establishment of gene expression signatures profiling the toxicity of environmental stressors.[12,13] Statistical methods used for DNA microarray studies are mostly multivariate approaches. Although basic methods treat genes as traits, which are consistent with the rules of experimental design, several approaches have been developed using expression ratio datasets. Such approaches regard the genes as cases and the array plates as variables. Most well-known methods based on singular value decomposition have used principal component analysis (Fig. 1).[14,15] In alternative approaches, our previous reports have described that a Bayesian network technique, which is a probabilistic graphical model that represents a set of variable identities, is applicable to investigation of the gene expression interaction networks and the detection of differences arising in them from exposure to different doses of chemicals.[16,17] Bayesian network techniques can provide predictive information related to the relations between agents and gene expression signatures in life science fields.[18–20]

Toyokuni[21] first proposed a new science field – oxygenomics – which is defined as a research area

Table 2 Core oxidative stress pathways

Categorical pathway Canonical pathway (orthology)
Reactive oxygen species (ROS) metabolism and antioxidant defenses
• Glutathione peroxidases (GPx)
• Peroxiredoxins (TPx)
• Superoxide dismutases (SOD)
• Genes involved in superoxide metabolism
• Genes involved in ROS metabolism
• Other peroxidases and antioxidant-related genes
p53 signaling (including DNA damage)
• Apoptosis-related genes
• Cell cycle arrest and checkpoint
• Regulation of the cell cycle
• Regulation of cell proliferation, cell growth and differentiation
• Damaged DNA binding
• Mismatch, base-excision and double-strand break repair
Nitric oxide (NO) signaling pathway
• Genes with NO synthase and regulators of NO biosynthesis
• Genes regulated by NO and NO signaling pathway
• Genes involved in superoxide release
• Anti-apoptosis genes
• Genes with antioxidant and superoxide dismutase activity
• Genes with glutathione peroxidase, oxidoreductase, peroxidase activity
• Transcription regulators
Hypoxia signaling
• Response to hypoxia and signal transduction, oxidative stress
• Genes related to stress and immune response
• Hemoglobin complex associated Genes
• Peroxidase, oxidoreductase-related genes
• Transcription factors and regulators and protein binding
• Anti-apoptosis
• Induction of apoptosis and caspase activity
• Protein biosynthesis, phosphorylation and metabolism
• Cytoskeleton and other extracellular molecules
• Cell cycle, cell proliferation and growth factors
• Carbohydrate, lipid, one-carbon compound metabolism
• RNA metabolism
• Cardiac excitation–contraction (E–C) coupling
TGF-β-BMP signaling
• TGF-β superfamily, bone morphogenetic protein (BMP) family members, growth differentiation factor (GDF), activin, and activin receptors
• SMAD family members, TGF-β/activin-responsive genes, BMP-responsive genes, molecules regulating signaling of the TGF-β superfamily, adhesion molecules, extracellular matrix structural constituents, other extracellular molecules, transcription factors and regulators
Tumor necrosis factor (TNF) ligand–receptor signaling
• Caspase activation, caspase inhibition, anti-apoptosis genes, induction of apoptosis, other apoptosis-related genes, JNK signaling pathway, NF-κB signaling pathway, TNF superfamily members, TNFr1 and TNFr2 signaling pathway, inflammatory response, transcription regulators
Mitochondria
• Mitochondrial processing, mitochondrial transportation, fatty acid biosynthesis

studying the localization of oxidative DNA damage in the genomes of living cells. Oxygenomics is becoming a significant strategy for discovery of important biomarkers and for evaluation of risks and effects.

This review addresses various environmental stressor-induced toxicities in rats and humans to elucidate the molecular mechanisms underlying toxicity-induced oxidative stress.

Categorical pathways in oxygenomics

Cells respond and adapt to environmental signals, such as stressors,[22–24] through multiple mechanisms that involve communication pathways and signal transduction processes. The impact of oxidative stress on various diseases and aging has been reviewed comprehensively. In particular, free-radical-induced oxidative stress plays an important role in cancer development, aging, and some toxicant-induced apoptosis.[3,25,36] Our survey of microarray databases and many other published references has revealed the categorical pathways induced by oxidative stress, as presented in Table 2.

ROS metabolism and antioxidant defenses center upon ROS, which are necessary for biological functions and which regulate many signal transduction pathways by directly reacting with and modifying the structure of proteins, transcription factors, and genes to modulate their functions. Actually, ROS induce expression levels of genes associated with signaling cell growth and differentiation, regulating the activity of enzymes (such as ribonucleotide reductase and peroxidase). Control of ROS levels is achieved by balancing ROS generation with their elimination through ROS-scavenging systems such as superoxide dismutases (SOD1, SOD2, and SOD3), glutathione peroxidase, peroxiredoxins, glutaredoxin, and thioredoxin catalase. The ROS can modulate the activities and expression of many transcription factors and signaling and signaling proteins that are involved in stress response and cell survival through multiple mechanisms. Therefore, this category includes glutathione peroxidases (GPx), peroxiredoxins (TPx), superoxide dismutases (SOD), genes involved in superoxide metabolism such as arachidonate 12-lipoxygenase (ALOX12), and copper chaperone for superoxide dismutase (CCS). In fact, p53 signaling plays a central role in co-ordinating the cellular responses to a broad range of cellular stress factors: p53 functions as a node for organizing whether the cell

responds to various types and levels of stress with apoptosis, cell cycle arrest, senescence, DNA repair, cell metabolism, or autophagy. Moreover, p53 controls *trans*-activation of target genes, which is an essential feature of stress response pathways.[37–39] In other words, p53 activation leads to a complicated network of responses to the various stress signals encountered by cells.[40–44] The mitochondrial respiratory chain produces nitric oxide (NO), which can generate other reactive nitrogen species (RNS) when cells are under hypoxic conditions. Although excess ROS and RNS can engender oxidative and nitrosative stress, moderate-to-low levels of both function in cellular signaling pathways. Especially important are the roles of these mitochondria-generated free radicals in hypoxic signaling pathways, which have important implications for cancer, inflammation, and various other diseases.[25,45] Hypoxic signaling events include vasodilation, modulation of mitochondrial respiration, and cyto-protection following ischemic insult. These phenomena are attributed to the reduction of nitrite anions to nitric oxide if local oxygen levels in tissues decrease,[46] which activates the expression of genes through oxygen-sensitive transcription factors including HIF and NF-κB. Hypoxia-dependent gene expression can have important physiological or pathophysiological consequences for an organism, depending upon the cause of the hypoxic insult.[47] These NO signaling and hypoxia signaling pathways are linked to the p53 pathway,[48] because recent studies have shown that HIF2α inhibition promotes p53-mediated responses by disrupting cellular redox homeostasis, thereby permitting ROS accumulation and DNA damage.[49] Reportedly, hypoxia activates the tumor suppressor protein p53 by up-regulating Sema3E expression.[50]

TGF-β-BMP signaling is involved in developmental morphogenesis and cancer morphogenesis. Morphogens such as those of the TGF-β family inhibit and stimulate basic cell proliferation, respectively, at high and low concentrations. A signaling gradient of declining TGF-β concentration regulates the inhibition and stimulation of cell proliferation.[51] Reactive oxygen species (ROS) can activate TGF-β either directly or indirectly via the activation of proteases. In addition, TGF-β itself induces ROS production as part of its signal-transduction pathway. Pulmonary tissues are vulnerable to the toxic effects of inhaled air. The oxidant pathways are especially relevant in the lung, where TGF-β is known to have a role in tissue repair and connective tissue turnover. In pulmonary fibrosis and renal endothelial cells, TGF-β activation is considered as a hallmark of disease progression.[52–53] In ovarian cancer, over-expression of FOXG1 contributes to TGF-β resistance through inhibition of p21WAF1/CIP1 expression, which is repressed by p53.[54] Tumor necrosis factor (TNF) ligand–receptor signaling occurs because TNF, as a multifunctional cytokine, can induce cell death through receptor-mediated caspase activation and mitochondrial dysfunction by a trigger of oxidative stress induced in cardiovascular disease, neuronal disease, and cancer.[55] Opposing these cell death-promoting signals, binding of TNF receptors can also trigger survival signal activation. A critical balance among various intracellular signaling pathways determines the predominant *in vivo* bioactivity of TNF, as best exemplified by the differential responses of various organs.

A major source of ROS in cells is the mitochondria. Electron leakage from the mitochondrial respiratory chain can react with molecular oxygen, resulting in the formation of the superoxide anion radical, which can subsequently be converted to other ROS. In phagocytes and some cancer cells, ROS are producible through a reaction that is catalyzed by NADPH oxidase complexes. When attackers from the outside, such as environmental stressors, damage mitochondria, electron leakage is also induced; this dysfunction induces severe problems in tissues.[56–59] Mitochondrial dysfunction causes the onset of some diseases.[60–63] Recent evidence has shown that mitochondrial dysfunction is related closely to insulin resistance and metabolic syndrome. The underlying mechanism of mitochondrial dysfunction is very complex, including genetic factors from both the nucleus and mitochondrial genome, with numerous environmental factors also impacting.[64]

Exposure to air pollution, including particles, metals, and other organic compounds as environmental stressors, is associated with pulmonary diseases and cancer. The mechanisms of induced health effects are believed to involve oxidative stress. Oxidative stress mediated by airborne particles and/or fibers might arise from direct generation of ROS from the surfaces of particles and fibers, soluble compounds such as transition metals or organic compounds, and activation of inflammatory cells capable of generating ROS and RNS. Generation of ROS/RNS can cause covalent modifications to DNA directly or they can initiate the formation of genotoxic lipid hydroperoxides. The resulting oxidative DNA damage can engender changed gene expression such as up-regulation of tumor promoters and down-regulation of tumor suppressor genes; the DNA damage might, therefore, be implicated in cancer development. This review describes the important role of free radicals in particle- and fiber-induced cellular damage, the interaction of ROS with target molecules, especially with DNA, and the

modulation of specific genes and transcription factor caused by oxidative stress. Consequently, various environmental stressors cause cellular damage through oxidative stress induction and many signaling pathways. However, what environmental stressor is dominant in which signaling pathway is not always clear. Therefore, identifying gene expression signatures extracted from microarray data can clarify how environmental stressors may damage cells and engender diseases.

Oxidative stress responsiveness in different conditions in rats

From the Gene Expression Omnibus (GEO; <http://www.ncbi.nlm.nih.gov/gds>), 33 independent microarray gene expression data with the same platform GPL341 (Affymetrix) sets in rats were downloaded for this study. All datasets were normalized across all arrays using Z-score transformation methods after combination with respect to probe IDs. The normalized values were filtered with oxidative-related genes listed in this work (see Supplement T2) and then the top 10 genes from up-regulated and down-regulated genes were chosen to analyze gene expression signatures (Table 3). The selected genes were classified using principal component analysis to create gene expression signatures of oxidative stress, and were divided into six groups. Most selected genes could be assigned to gene ontology (GO) categories: DNA repair, oxygen and reactive oxygen species metabolism, and response to stress, but cyclins and cyclin-dependent kinase contained in 'Apoptosis related genes, Cell Cycle Arrest and Checkpoint, Regulation of the Cell Cycle, Regulation of Cell Proliferation, Cell Growth and Differentiation' of 'p53 signaling' and 'TGF-beta signaling' were not observed. Experimental conditions selected from GPL341 datasets in this work were almost all of short-period exposure using *in vivo* and *in vitro* culture systems of rats. It is noteworthy that microarrays capture only transient responses to oxidative stimuli. However, we can predict the underlying mechanism of environmental stressors through oxidative signatures for gene expression. For example, in cluster 1 (GDS964,[65] GDS972,[66] GDS1393,[67] GDS2555,[68] GDS2558,[69]), GPXs, NOS, and NOX were up-regulated, suggesting that environmental stessors in the cluster 1 can activate the NO signaling that leads to inflammation or other cellular damage. Thioredoxin interacting protein, Txnip, was identified as a unique gene in this category. In cluster 2 (GDS696,[70] GDS880,[71] GDS1518,[72] GDS1626,[73] GDS2107,[74] GDS2372,[75] GDS2457,[76] GDS2688[77]), Rad23, Rad50, Rad51c, which are DNA repair and recombination proteins, and the other DNA replication proteins DNA-directed DNA polymerase delta (Pold)1 and Pold3 were classified. This classification suggests that environmental stressors in cluster 2 such as fibronectin, protein restriction, heregulin, kainic acid, hypoxia and ethanol harmed mitochondria or damaged DNA more than the stressors in cluster 1. In cluster 3 (GDS1363,[78] GDS1452[79], GDS1922,[80] GDS2037,[81] GDS2073,[82] GDS2093,[83] GDS 2194,[84], GDS2616,[85] GDS2639,[86] GDS2774,[87] GDS2901,[88] GDM1038,[89]), Gadd45a, Nthl1, Mgmt, Mpp4, Chek1 Cry2, Txnrd1 were observed as up-regulated genes. Since these genes interact with DNA repair and p53 signaling activated, it is possible that environmental stressors in the cluster 3 cause DNA damage and remodeling. In cluster 4 (GDS902,[90] GDS2243,[91] GDS2361,[92]), DNA replication proteins Pinx1 and Slk were detected as unique genes. Especially, STE20-like kinase (Slk) appears to influence cell survival and proliferation. In fact, Slk has been suggested to have a central growth-suppressive role for Mst orthologs, with intriguing possible links to other established tumor suppressors through work in model organisms. Some of the genes in cluster 5 (GDS1027,[93] GDS1273,[94] GDS1959[95]) overlapped with clusters 1 and 3. In cluster 6 (GDS1354,[96] GDS2231[97]), some genes overlapped with clusters 2 and 4. However, Vim was detected as a unique gene in GDS1354, which is an experiment in cirrhotic rats,[96] and up-regulation of this gene was also observed in renal cell carcinoma,[98] cerebral tumors,[99] germ cells, and trophoblastic neoplasms.[100]

Oxidative stress-induce gene expression signatures in human tissues

Among many oxidative responsive pathways, p53 signaling has been studied extensively and has been thought to play a main role in the orchestration of oxidative events in cells. It co-ordinates the cellular responses to a broad range of cellular stress factors. In fact, p53 functions as a node for organizing whether the cell responds to various types and levels of stress with apoptosis, cell cycle arrest, senescence, DNA repair, cell metabolism, or autophagy, as described earlier in this review.[37–39] To control and fine-tune responses to various stress signals encountered by cells, as a transcription factor that both activates and represses a broad range of target genes, p53 demands an exquisitely complicated regulatory network. The

Table 3 The top 10 up-regulated and down-regulated genes in the clusters analyzed

Cluster	GEOID	Environmental stressors (target organ or tissues)	Up-gene	Down-gene
1	GDS964	Methylprednisolone (kidney)	Apoe, Gpx2, Ngb, Nos2, Prdx6, Tmod1, Tnp1, Tpo	Brca2, Cry2, Fen1, Hus1, Ptgs2, Pttg1, Rad50, Srxn1, Xrcc6
	GDS972	Methylprednisolone (liver)	Aass, Atrx, Ncf1, Nqo1, Scd1, Slc41a3, Srd5a2, Tmod1, Tnp1	Chek1, Cry2, Lig1, Mgmt, Pold1, Pold3, Rad50, Rad52, Smc3, Xrcc6
	GDS1393	Streptozotocin (penile cavernosal)	Apc, Cat, Duox2, Gpx2, Gpx6, Gsr, Lpo, Slc38a1, Smc3, Tpo	Atrx, Gpx7, Nos2, Park7, Ptgs2, Scd1, Slc38a4, Slc41a3, Srxn1, Zmynd17
	GDS2555	Trimethyltin (hippocampus)	Apex1, Dnm2, Fancc, Gpx7, Lpo, Mgmt, Park7, Prnp, Txnip, Ucp3	Apc, Apoe, Hbz, Mpp4, Ptgs2, Smc3, Srd5a2, Tnp1, Tpo
	GDS2558	Octreotide (gastric ECL)	Brca1, Brca2, Dnm2, Duox2, Msh2, Nox4, Tmod1, Tpo, Xirp1	Apex1, Atrx, Cry2, Gpx6, Nos2, Slc38a1, Slc38a4, Slk, Tmod1, Tpo
2	GDS696	Fibronectin (ventricular myocytes)	Apoe, Atrx, Chaf1a, Ngb, Rad51c, Smc3, Srxn1, Tpo, Zmynd17	Actb, Atrx, Gsr, Mutyh, Ngb, Prdx6, Rad52, Smc3, Tpo, Txnrd1
	GDS880	Protein restriction (visceral adipose tissue)	Aass, Apc, Gpx6, Gstk1, Ngb, Prnp, Rad51c, Scd1, Tmod1, Tnp1	Brca2, Chaf1a, Lpo, Mutyh, Nos2, Pttg1, Slc38a1, Slc38a4, Tpo, Ung
	GDS1518	Heregulin (ureteric buds)	Dhcr24, Hus1, Ldha, Mif, Park7, Rad1, Rad50, Scd1, Tdg, Ung	Actb, Atrx, Nos2, Nox4, Nqo1, Ptgs1, Rad23a, Srxn1, Txnrd1
	GDS1626	Kainic acid (hippocampi)	Apoe, Brca2, Ncf1, Nox4, Pold1, Rad23a, Rad50, Rad51c, Srd5a2, Tmod1	Chaf1a, Hbz, Lpo, Mb, Pold3, Tnp1, Tpo, Ucp3, Ung, Zmynd17
	GDS2107	Ethanol (pancreas)	Apoe, Atrx, Hbz, Ogg1, Ptgs2, Scd1, Srxn1, Tmod1, Txnrd2, Zmynd17	Cry2, Hus1, Mb, Msh2, Nox4, Nthl1, Prdx6, Rad52, Slk, Srd5a2
	GDS2372	Sulfur dioxide (lung)	Aass, Brca1, Cry2, Hus1, Nos2, Ptgs2, Pttg1, Rad50, Tpo, Zmynd17	Apex1, Brca2, Gpx6, Nos2, Nox4, Rad23a, Rad51c, Srd5a2, Tnp1, Tpo
	GDS2457	Hypoxia (adrenal gland)	Chaf1a, Duox2, Ldha, Ngb, Pold3, Rad23a, Slc41a3, Tpo, Txnrd2	Aass, Apc, Apoe, Atrx, Cry2, Lpo, Nox4, Rad52, Srd5a2, Tnp1
	GDS2688	Methylprednisolone (skeletal muscles)	Aass, Atrx, Hbz, Ngb, Rad1, Scd1, Slc38a5, Tmod1, Tpo, Xirp1	Als2, Atrx, Brca2, Cat, Gsr, Ncf1, Nox4, Nqo1, Slc41a3, Trpc2
3	GDS1363	Forskolin (pheochromocytoma cell)	Aass, Apex1, Brca1, Chek1, Duox2, Gpx2, Hbz, Nxn, Ptgs1, Pttg1	Atrx, Cat, Cygb, Ehd2, Gpx3, Gpx4, Gpx7, Scd1, Sod3, Vim
	GDS1452	N-methyl-N-nitrosourea (mammary tumors)	Cat, Ehd2, Gadd45a, Gstk1, Mgmt, Prdx3, Prdx6, Scd1, Srxn1, Ube2a	Dpagt1, Gab1, Gpx3, Lpo, Mpg, Nxn, Prdx4, Prnp, Rad52, Txnip
	GDS1922	Retinoic X receptor ligand LG100268 (mammary gland)	Brca1, Dnm2, Gpx6, Hbz, Mpp4, Ncf1, Nos2, Slc38a1, Tpo	Aass, Atrx, Chaf1a, Gsr, Idh1, Nox4, Prdx1, Rad23a, Xrcc1, Zmynd17
	GDS2037	Angiopoietin-1 (aortic rings)	Apex1, Dnm2, Mgmt, Ngb, Pold3, Rad50, Slc38a1, Srd5a2, Srxn1, Ucp3	Atrx, Brca2, Chaf1a, Gpx6, Mb, Nox4, Rad23a, Slk, Tpo, Zmynd17
	GDS2073	Isoflurane (basolateral amygdalae)	Brca2, Gpx2, Ift172, Mif, Nos2, Pttg1, Rad1, Rad51c, Tpo, Ung	Atrx, Atrx, Gsr, Nox4, Pold3, Prnp, Ptgs2, Scd1, Smc3, Xrcc6
	GDS2093	Fe-deficiency (jejunum)	Aass, Gadd45a, Gsr, Nqo1, Srxn1, Tdg, Tmod1, Txnrd1, Xrcc1,	Gpx7, Hba-a2, Lpo, Mgmt, Nthl1, Pms2, Rad52, Smc3, Xpc, Xrcc6
	GDS2194	Pregnenolone16alpha-carbonitrile (liver)	Dnm2, Gpx6, Lpo, Nqo1, Prdx5, Ptgs2, Scd1, Srxn1, Tpo, Txnrd1	Aass, Als2, Apoe, Hbz, Nos2, Rad51c, Slc38a5, Srd5a2, Tpo
	GDS2616	Particulate matter (TPM)/l of cigarette smoke (lung)	Aass, Apc, Brca1, Brca2, Cry2, Gpx2, Hus1, Slc38a4, Tpo, Txnrd1	Chaf1a, Mb, Mutyh, Nos2, Pold3, Ptgs2, Rad50, Tmod1, Tnp1, Tpo
	GDS2639	Genistein (mammary epithelial cells)	Atrx, Brca2, Hba-a2, Ngb, Rad23a, Rad52, Smc3, Tpo, Ung, Zmynd17	Apex1, Brca1, Gpx6, Lpo, Pttg1, Slc38a4, Srd5a2, Tnp1, Tpo
	GDS2774	Aging (hippocampi)	Atrx, Ehd2, Gadd45a, Gtf2h1, Mgmt, Ncf1, Nthl1, Ptgs2, Pttg1, Srxn1	Ercc6, Mlh1, Pms2, Rad50, Rad52, Slc38a1, Trpc2, Txnip, Wrnip1, Xpc
	GDS2901	Depolarization. (midbrain)	Apc, Apoe, Atrx, Brca1, Pold3, Ptgs2, Rad23a Slc38a4, Smc3, Zmynd17	Apex1, Atrx, Chaf1a, Gpx2, Hba-a2, Nos2, Pttg1, Srxn1, Tmod1, Tnp1
	GSM1038	Aristolochic acid (kidney)	Apoe, Atrx, Cry2, Ngb, Ppp1r15b, Scd1, Srxn1, Tpo	Apoe, Atrx, Fen1, Gadd45a, Gpx6, Ift172, Pold3, Rad52, Txnip, Zmynd17
4	GDS902	Pyridine activator (ventricular myocytes)	Aass, Chaf1a, Dhcr24, Nthl1, Pinx1, Pold3, Rad52, Scd1, Slc38a1, Xirp1	Apex1, Brca2, Cry2, Gpx6, Hus1, Lpo, Mutyh, Pold1, Rad51c, Tpo
	GDS2243	Re-innervation (tibialis anterior muscles)	Apex1, Atrx, Chek1, Gpx6, Mgmt, Ncf1, Nox4, Pold3, Smc3, Tnp1	Atrx, Brca1, Chaf1a, Lpo, Nthl1, Rad50, Slc41a3, Txnrd2, Ung, Zmynd17
	GDS2361	Hyperinsulinemia (kidney)	Apoe, Chaf1a, Gpx6, Hba-a2, Lpo, Ngb, Ptgs2, Scd1, Slk, Srd5a2	Apc, Atrx, Duox2, Hbz, Mb, Ncf1, Slc38a4, Tmod1, Tnp1, Txnip

Table 3 (cont'd) The top 10 up-regulated and down-regulated genes in the clusters analyzed

Cluster	GEOID	Environmental stressors (target organ or tissues)	Up-gene	Down-gene
5	GDS1027	Sulfur mustard *bis*-(2-chloroethyl) sulfide (lung)	Apoe, Gadd45a, Gpx2, Hba-a2, Mif, Prdx5, Ptgs2, Scd1, Smc3, Srxn1	Apc, Atrx, Dnm2, Duox2, Gab1, Gpx6, Mutyh, Nox4, Srd5a2, Tpo
	GDS1273	Amoxicillin (intestine)	Apc, Apoe, Atrx, Lpo, Mutyh, Slc38a4, Tnp1, Tpo	Apex1, Chaf1a, Cry2, Gpx2, Ngb, Nox4, Scd1, Tpo, Trpc2, Zmynd17
	GDS1959	Ischemia (heart)	Apc, Apoe, Gpx7, Nos2, Nox4, Nxn, Prdx4, Rad52, Scd1, Smc3	Atrx, Brca1, Chaf1a, Hus1, Lpo, Pold1, Prdx5, Rad51c, Slc38a4, Xirp1
6	GDS1354	Carbon tetrachloride (liver)	Chaf1a, Ehd2, Gpx2, Hba-a2, Ncf1, Prnp, Ptgs2, Slc38a4, Vim, Zmynd17	Apoe, Dpagt1, Gab1, Hus1, Nos2, Nxn, Ptgs1, Slk, Trpc2, Txnip
	GDS2231	Dexamethasone (marrow-derived stromal cells)	Apoe, Ehd2, Gpx6, Mgmt, Mpp4, Srd5a2, Tmod1, Tpo	Apex1, Apoe, Chaf1a, Dnm2, Nos2, Rad50, Rad51c, Slk, Smc1a, Smc3

classical model for activation of p53 specifically examines three simple and rate-limiting steps: p53 stabilization induced by ataxia telangiectasia mutated (ATM)/ataxia telangiectasia and Rad3 related (ATR)-mediated phosphorylation, sequence-specific DNA binding, and target gene activation through interaction with the general transcriptional machinery.[29] Recent studies with animal models describe that mouse double minute (Mdm) 2 and MdmX might determine whether a cell responds to p53 activation with growth arrest or apoptosis, but the molecular mechanism of these differential effects remains unknown. In fact, Mdm2 and MdmX can both be recruited to p53 promoter regions. Via a multitude of mechanisms, they can repress transcription of p53 target genes.[101–103] The p53 protein binds sequence-specific regions of DNA of the target gene to process sensing and removal of oxidative damage to nuclear DNA and genetic instability. Furthermore, p53 acts as a transcription factor to regulate the expression of many pro-oxidant and antioxidant genes. A new refined model for p53 activation includes three key steps: (i) p53 stabilization; (ii) anti-repression; and (iii) promoter-specific activation. Among the three steps, most environmental stressors contribute mainly to p53 stabilization and promoter-specific activation. Several reports describe that small weight molecules engender induction of stress-induced genes such as NAD(P)H dehydrogenase, quinone (NQO)1 and NQO2, which stabilize and transiently activate p53 and downstream genes leading to protection against adverse effects of stressors.[104–106]

Therefore, to understand how stress-induced genes are downstream within the p53 pathway, we analyzed gene expression of p53 signaling pathways in array datasets GDS2780[107] and GSE7967[108] that had been obtained from the GEO database. In the GDS2780 study, six heavy metals and three organic compounds that were exposed in liver carcinoma HepG2 cells (Fig. 2A) responded dramatically to gene expression of CHK1, CHK2, Cyclin B Cdc2 p21, p53R2, Cop1-1, and Gadd45. Interestingly, expression levels of p53R2 and Gadd45 responded differently to the heavy metals: p53R2 is likely to associate with mitochondrial DNA and play a critical role in embryogenesis and neurogenesis;[109–113] in contrast, Gadd45 plays a vital role as a cellular stress sensor in the modulation of cell signal transduction in response to stress. Increasing Gadd45 can stabilize p53 activation, leading to cell cycle arrest or procession to apoptosis.[114–116] Consequently, exposure of cultured human cells to heavy metals dramatically altered the gene expression of oxidative-responsive genes. However, in human tissues of the GSE7967 study, the p53 signaling pathway differed from that of heavy metals in the GDS2780 study. Overall, the gene expression signals were weaker than those examined in the GDS2780 study. The GSE7967 study examined cord blood collected at birth from infants whose mothers were exposed or unexposed to arsenic (0.1–68.63 mg/g), showing activation of inflammation and NF-κB signaling in infants born to mothers exposed to arsenic at high concentration. Therefore, after downloading the datasets, we selected four subjects according to blood concentrations of 0.1, 1.76, 9.66, and 68.63 mg/g; then, gene expression of the arsenic (As) exposure-induced responses were visualized in the p53 signaling pathway map (Fig. 2B). The highest concentration subject showed Gadd45, p53-inducible ribonucleotide reductase small subunit 2 (p53R2), spermatogenic leucine zipper 1 (TSP1), cyclinB, Cdc2, Fas, Noxa and ATR that were higher than those of the subject with the low concentration. However, p53 was opposite: high in the low-exposure subject and low in the high-exposure subject, suggesting that the down-regulation of p53 facilitates apoptosis and promotes cell proliferation.

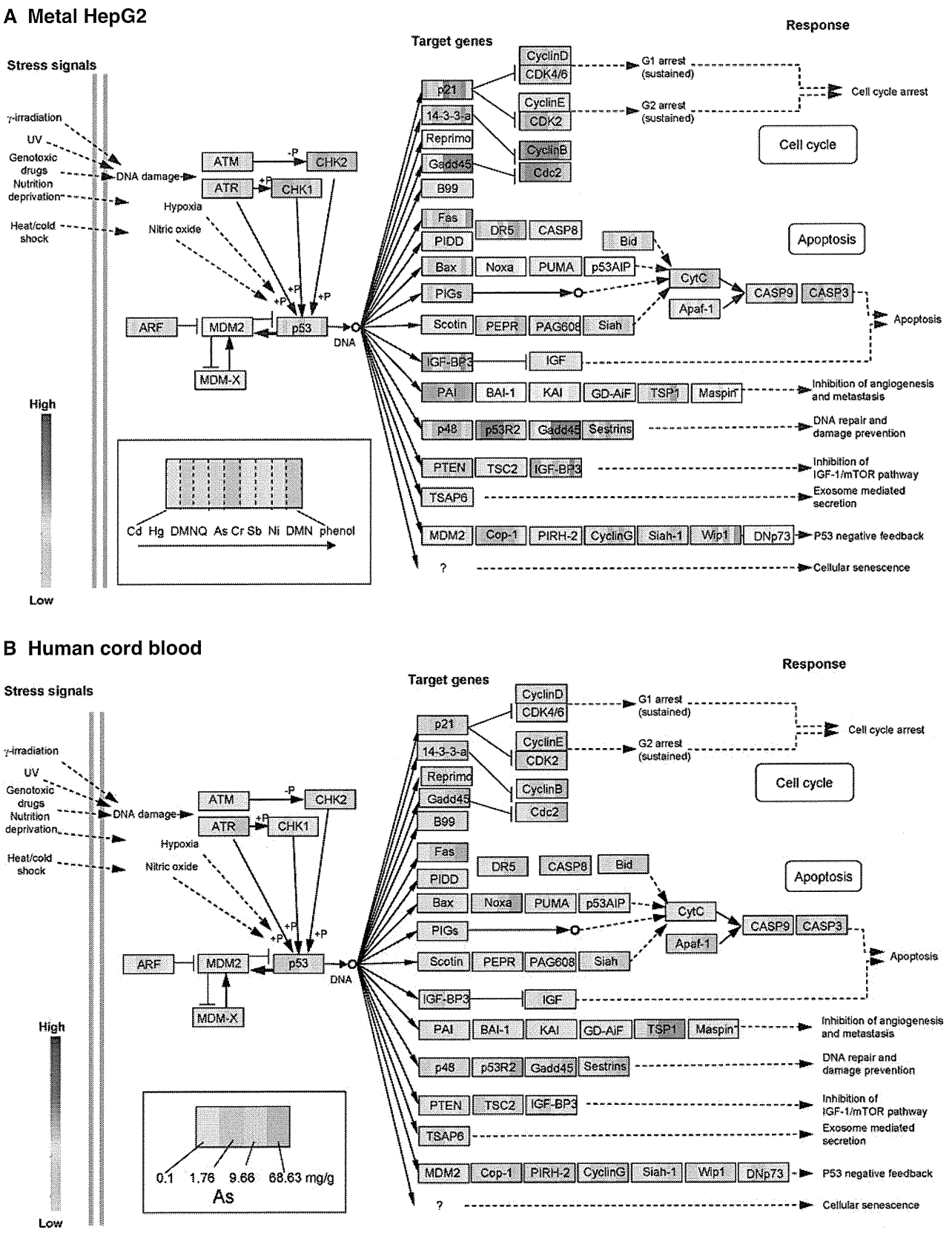

Figure 2 Oxidative gene signature in the p53 signaling pathway pathway in array datasets GDS2780[107](A) and GSE7967[108](B). (A) Heavy metals and organic compounds used in the HepG2 study. Gene expression levels in each box corresponding to each gene symbol are aligned from the left as Cd, Hg, 2,3-dimethoxy-1,4-naphthoquinone (DMNQ), As Cr, Sb, Ni, and DMN, phenol. (B) Human umbilical cord blood. Gene expression levels presented from the left are for 0.1, 1.76, 9.66, and 68.63 mg/g blood arsenic concentration

Previous works described in our study showed that GSS (glutathione synthetase) and PRDX2 (peroxiredoxin 2) regulated TNF receptor-1 associated protein (TRADD), nucleoside diphosphate linked moiety X-type motif 1 (NUDT1), SOD1, and insulin induced gene 1 (INSIG1) in the low-exposure group (mean blood concentration 0.142 μg/g), and that NUDT1 regulated TRADD, TXNRD2, and PRDX2 in the high-exposure group (21.41 μg/g) using the theoretical algorithm for identifying optimal gene expression networks (TAO-Gen), which is a Bayesian network algorithm used to describe gene interaction networks.[17,117–119] In fact, NUDT1 is a DNA repair and recombination protein. The H_2O_2 treatment significantly increased this gene and other oxidative-stress genes involved in cell cycle arrest.[120] Results of our analyses suggest that anti-oxidative stress-related genes play key roles in protection against cellular damage in the low-exposure group, but a DNA damage-related gene was dominant in the high-exposure group, in which cell damage would progress. In addition, TGF-β and TNF signaling were not strongly respondent in this re-analysis, although another paper has described pathways that are shared by oxidatively stressed and early-onset breast cancer associated interactions between TGF-β and TNF signaling.[121] Datasets used in this review are fundamental exposure to environmental stressors in normal tissues and cell lines, Therefore, this discrepancy indicates that gene expression signatures in human clinical tissues or epidemiological studies apparently reflect more inflammation than those of experimental materials, which show acute toxicity in animals after short exposure to oxidants in cell cultures.

Conclusions

Herein, based on recent advances, we surveyed gene expression signatures of environmental stressor-induced oxidative stress and proposed categorical pathways and canonical pathways of oxidative stress in rodent and human systems. Analyses of gene expression signatures in environmental related disease such as neuronal disorders, cancer and diabetes is an important approach in etiology and risk assessment for human health to elucidate the underlying mechanisms of induced health effects. Although we did not survey anti-oxidative stress responses induced by environmental stressors in this review, anti-oxidation systems such as the NRF2-keap1 system should be discussed for association with p53 pathways in an other review. This will take many more genetic and reverse genetic analyses, combined with functional analysis studies. Helped by complementary analyses in environmental stressor or environmental stressor-related disease, we expect soon to see the first attempts to predict influences induced by environmental stressors, taking into account the wealth of experimental data gathered. Although this might uncover interesting feed-forward and feed-back mechanisms, it will take more time to link these signaling interactions to the cell behaviors that control the different aspects of oxygenomics discussed here. It is important to realize that oxygenomics is integral to profiling effects of environmental stressors, which all need to be further classified in this way.

References

1. Gibb S. Toxicity testing in the 21st century: a vision and a strategy. *Reprod Toxicol* 2008; **25**: 136–138.
2. Woods CG, Heuvel JP, Rusyn I. Genomic profiling in nuclear receptor-mediated toxicity. *Toxicol Pathol* 2007; **35**: 474–494.
3. Franco R, Panayiotidis MI. Environmental toxicity, oxidative stress, human disease and the 'black box' of their synergism: how much have we revealed? *Mutat Res* 2009; **674**: 1–2.
4. Hansen JM, Zhang H, Jones DP. Differential oxidation of thioredoxin-1, thioredoxin-2, and glutathione by metal ions. *Free Radic Biol Med* 2006; **40**: 138–145.
5. Valko M, Rhodes CJ, Moncol J, Izakovic M, Mazur M. Free radicals, metals and antioxidants in oxidative stress-induced cancer. *Chem Biol Interact* 2006; **160**: 1–40.
6. Bau DT, Wang TS, Chung CH, Wang AS, Wang AS, Jan KY. Oxidative DNA adducts and DNA-protein cross-links are the major DNA lesions induced by arsenite. *Environ Health Perspect* 2002; **110 (Suppl 5)**: 753–756.
7. Kawai Y, Furuhata A, Toyokuni S, Aratani Y, Uchida K. Formation of acrolein-derived 2'-deoxyadenosine adduct in an iron-induced carcinogenesis model. *J Biol Chem* 2003; **278**: 50346–50354.
8. Chiu HJ, Fischman DA, Hammerling U. Vitamin A depletion causes oxidative stress, mitochondrial dysfunction, and PARP-1-dependent energy deprivation. *FASEB J* 2008; **22**: 3878–3887.
9. Knott L, Hartridge T, Brown NL, Mansell JP, Sandy JR. Homocysteine oxidation and apoptosis: a potential cause of cleft palate. *In Vitro Cell Dev Biol Anim* 2003; **39**: 98–105.
10. Nebert DW, Petersen DD, Fornace Jr AJ. Cellular responses to oxidative stress: the [Ah] gene battery as a paradigm. *Environ Health Perspect* 1990; **88**: 13–25.
11. Cheng Y, Chang LW, Cheng LC, Tsai MH, Lin P. 4-Methoxyestradiol-induced oxidative injuries in human lung epithelial cells. *Toxicol Appl Pharmacol* 2007; **220**: 271–277.
12. Mendrick DL. Genomic and genetic biomarkers of toxicity. *Toxicology* 2008; **245**: 175–181.
13. Luhe A, Suter L, Ruepp S, Singer T, Weiser T, Albertini S. Toxicogenomics in the pharmaceutical industry: hollow promises or real benefit? *Mutat Res* 2005; **575**: 102–115.
14. Wall ME, Dyck PA, Brettin TS. SVDMAN – singular value decomposition analysis of microarray data. *Bioinformatics* 2001; **17**: 566–568.
15. Yeung KY, Ruzzo WL. Principal component analysis for clustering gene expression data. *Bioinformatics* 2001; **17**: 763–774.
16. Portier CJ, Toyoshiba H, Sone H, Parham F, Irwin RD, Boorman GA. Comparative analysis of gene networks at multiple doses and time points in livers of rats exposed to acetaminophen. *Altex* 2006; **23 (Suppl)**: 380–384.